New Jersey Institute of Technology

Digital Commons @ NJIT

Spring 5-31-2000

Development and characterization of techniques for neuro-imaging registration

Carlo Ciulla
New Jersey Institute of Technology

Follow this and additional works at: https://digitalcommons.njit.edu/theses

Part of the Databases and Information Systems Commons, and the Management Information Systems Commons

ABSTRACT

DEVELOPMENT AND CHARACTERIZATION
OF TECHNIQUES FOR
NEURO-IMAGING REGISTRATION

by
Carlo Ciulla

Three automated techniques were developed for the alignment of Neuro-Images acquired during distinct scanning periods and their performance were characterized. The techniques are based on the assumption that the human brain is a rigid body and will assume different positions during different scanning periods. One technique uses three fiducial markers, while the other two uses eigenvectors of the inertia matrix of the Neuro-Image, to compute the three angles (pitch, yaw and roll) needed to register the test Neuro-Image to the reference Neuro-Image. A rigid body transformation is computed and applied to the test Neuro-Image such that it results aligned to the reference Neuro-Image. These techniques were tested by applying known rigid body transformations to given Neuro-Images. The transformations were retrieved automatically on the basis of unit vectors or eigenvectors. The results show that the precision of two techniques is dependent on the axial resolution of the Neuro-Images and for one of them also on the imaging modality, while the precision of one technique is also dependent on the interpolation. Such methods can be applied to any Neuro-Imaging modality and have been tested for both fMRI and MRI.

DEVELOPMENT AND CHARACTERIZATION
OF TECHNIQUES FOR
NEURO-IMAGING REGISTRATION

by
Carlo Ciulla

A Thesis
Submitted to the Faculty of
New Jersey Institute of Technology
In Partial Fulfillment of the Requirements for the Degree of
Master of Science in Information Systems

Department of Computer and Information Science

May 2000

APPROVAL PAGE

DEVELOPMENT AND CHARACTERIZATION

OF TECHNIQUES FOR

NEURO-IMAGING REGISTRATION

Carlo Ciulla

Dr. Fadi P. Deek, Thesis Advisor.   Date
Vice Chairperson and Associate Professor of Computer Information Science,
NJIT - New Jersey Institute of Technology, Department of Computer Information
Science, Newark 07102 NJ.

Dr. Benjamin Martin Bly, Thesis Co-Advisor.   Date
Assistant Professor of Cognitive Psychology,
RUTGERS - The State University of New Jersey, Department of Psychology,
Newark 07102 NJ.

Dr. Murray Turoff, Committee Member.   Date
Distinguished Professor of Computer and Information Science,
NJIT - New Jersey Institute of Technology, Department of Computer Information
Science, Newark 07102 NJ.

BIOGRAPHICAL SKETCH

Author: Carlo Ciulla

Degree: Master of Science in Information Systems

Date: May 2000

Undergraduate and Graduate Education:

- Master of Science in Information Systems,
  New Jersey Institute of Technology, Newark, NJ, 2000

- Bachelor and Master Degree in Management Engineering,
  University of Palermo, Faculty of Engineering, Palermo, Italy, 1994

Major: Information Systems

Presentations and Publications:

C. Ciulla, T. Takeda and H. Endo.
"MEG characterization of spontaneous Alpha Rhythm in the Human Brain." Brain Topography, Volume 11, Number 3. 1999.

C. Ciulla, T. Takeda, M. Morabito, H. Endo, T. Kumagai and R. Xiao.
"MEG measurements of 40Hz auditory evoked response in human brain." Supplement 47 to Electroencephalography and Clinical Neurophysiology. 1996.

C. Ciulla, T. Takeda and H. Endo.
"Temporal Analysis of Alpha Activity in Human Brain using a Whole-Head MEG System." The Journal of Japan Biomagnetism and Bioelectromagnetics Society Vol. 9 No.1. 1996.

C. Ciulla, T. Takeda, R. Xiao, M. Morabito, T. Kumagai and H. Endo.

"Temporal Analysis of Alpha Activity in Human Brain using a Whole-Head MEG System." BPES' 95 Proceedings of the 10th Symposium on Biological and Physiological Engineering. 1995.

To my mother Angela Parlavecchio

ACKNOWLEDGEMENT

TABLE OF CONTENTS

LIST OF FIGURES

LIST OF TABLES

CHAPTER 1

INTRODUCTION

1.1 Objective

Neuro-Image alignment is a problem that must be approached and solved in all techniques prior to any computational procedure aimed to analyze data. Presently, Neuro-Imaging techniques such as fMRI (functional Magnetic Resonance Imaging), MRI (Magnetic Resonance Imaging), PET (Positron Emission Tomography) and CT (Computerized Tomography), among others, require head movement correction. Correction of any head movements that may happen during scanning must be employed prior to any data analysis to avoid artifacts. Several automated methodologies have been applied in the past with relatively good success, [1], [17], [21], [24], [25]. Some of such methodologies rely on the assumption that the human brain is a rigid body subject to rigid motion during the period of scanning, [1], [21], [24], [25]. Another technique [17] assumes that head movement artifacts are still present after alignment is performed.

In this thesis are presented results obtained by implementing three techniques for Neuro-Image alignment. We have reproduced the principal axes transformation method [1], a similar technique that has been derived from it and we have implemented my own method derived from previous research [10], [11]. The three techniques rely on the assumption that the human brain is subject to rigid body motion during different scanning periods. On the basis of the rigid body assumption, it is possible to identify the position of the brain into the scanning

volume by a head coordinate system. Our technique uses three points (chosen as fiducial markers) and three coordinates (x, y and z) to determine the unit vectors of a head coordinate system on the basis of which the head position is featured within the scanning volume. The mathematical basis for this technique was successfully employed to co-registrate MRI with MEG during previous work that investigated the origin into the human brain of the spontaneous Alpha rhythm [10], and the 40 Hz Auditory steady state response [11]. The methods have been successfully implemented on a SGI Onyx 2 workstation and they consist of two software packages written under Matlab, Open GL and ANSI C.

1.2 The Problem

In many image processing applications it is necessary to form a pixel-by-pixel comparison of two images of the same object field obtained from different sensors, or two images of an object field taken from the same sensor at different times. To form this comparison, it was reported [23] that it is necessary to spatially register the images and thereby correct for relative translational shifts, magnification differences, and rotational shifts, as well as geometrical and intensity distortions of each image.

It was reported [2] an automatic algorithm with subpixel accuracy and it was applied to the registration of two-dimensional computed radiography (CR). The algorithm computed local correlation of pixel data between the reference image and the test image at specific regions of interest scattered through the images. The coordinates of the local correlation peaks were then fit by a last squares method to a rigid two-dimensional grid pattern to determine the angle, displacement and magnification differences between the two images. Another method based on correlation between the two images to be realigned, was described and applied [13] to a series of experiments with synthetic and real two-dimentional images of various type.

A general purpose representation-independent method for the accurate registration of 3-D shapes was reported [6]. The method handles the full six degree of freedom and it is based on an iterative closest point (ICP) algorithm. The algorithm, given an initial set of rotations and translations, globally minimize the mean-square distance metric over all six degree of freedom by testing each initial

registration.

In order to register a pair of images, an image registration algorithm often employs some similarity criterion between the image function, testing different displacement vectors to find an extremum of this similarity measure. It was introduced [8] a new similarity measure based on the number of coincidents bits in multichannel image applications. The algorithm used a coincident bit counting method to obtain the number of matching bits between the frames of interest and determine the translational motion among sequence of images derived from digital angiography and mammography. It was described [9] a method that uses Fourier magnitude and correlation coefficients as a similarity measure. The algorithm computed rotations translations and scaling and was applied to the registration of retinal images.

As far as fMRI data series are concerned, the problem is constituted by head movement artifacts. Despite restraints to inhibit head movement, even willing and co-operative subjects still show head displacements. With some subjects (i.e. very young) head restraints appear to be ineffective with this respect. In such circumstances, head movement of several millimeters is not uncommon [17]. Therefore, a head movement correction technique must be applied after fMRI data collection. Various techniques have been proposed in this regard. Next, the relevant literature is reviewed and the performance of the three techniques that have been implemented is evaluated.

1.3 Review of the Literature

A method reported in the past [21] described a surface matching technique to register multiple imaging scans (PET, CT and MRI) of the brain in three dimensions. This method was based on the following assumption: given two 3D models of an object, a unique coordinate tranformation can be found which, when applied to one of the models, makes the two fit together most closely. An algorithm developed earlier [22] was used for minimization of a non linear function of several variables to find the geometrical transformation that when applied to one of the models coordinates, minimizes a residual that is the mean squared distance between the one model's points and the other model's surface.

A computational technique called registration by the principal axes transformation was developed [1] a decade ago. This methodology assumed the brain to be a rigid body and was developed for the registration Neuro-Images which are rotated and translated in the transverse section plane. The performance of the method was studied with image data from PET, XCT and MRI. It was found that progressively, coarser sampling of data sets led to some degradation in the performance of the method.

A registration technique were described [24]-[25] which do not require fiducial markers. To align two images, the method calculates the ratio of one image to the other on a voxel-to-voxel basis and then iteratively moves the images relative to one another to minimize the variance of this ratio across voxels. Such a method was applied both for within modality registration of PET images, and for cross modality registration of MRI-PET images. The authors [24]-[25] provided an idea to solve

the problem of MRI-PET registration. A coordinate system solidal to the subject head was built both for PET and MRI. The coordinate system was obtained from two plexiglas plates with fiducial channels drilled into them in the shape of the letter N. The two plates were attached on a stereotaxic frame on the right and left sides of the patient's head. Constructing the above coordinate system both for MRI and PET images, realignment could be done with a sufficient degree of reliability [24].

Another approach [3] used an entropy focus criterion to determine unknown rigid-body patient motion in the imaging plane for Magnetic Resonance Images.

As far as fMRI realignment is concerned, techniques were reported [12] for automatically transform into stereotaxic coordinates (Talairach-Tournoux), anatomical and functional scans. The techniques relied on manual placement of markers on anatomical landmarks. It was reported [20] an image registration algorithm that decouples the estimation of interframe rotational and translational displacements and transforms each motion parameter into an independent linear shift, allowing the application of cross-correlation and cross-spectrum techniques for the estimation of the displacement parameters. The method was applied to functional MRI time series data. Techniques were reported [18]-[19] that can account for head motion that occurs through-plane and head rotation, by the use of navigator echos in fMRI. It was presented [14] a technique for performing two-dimensional rigid-body image registration for functional magnetic resonance images performing the computation of rotational and translational parameters in the Fourier domain.

It was shown [7] that intensity-based registration cannot accurately register two or more images in the precence of local intensity changes arising from functional Magnetic Resonance signals. Such research presented a countour based technique that can be used for a more robust registration and also to differentiate between task-induced and motion-induced signal changes. The correlation coefficient between the contour images of a given pair was initially computed and then the images were shifted until it became maximum.

It was reported [17] that simply moving the images back into register is not sufficient to remove the effects of the head movement. Therefore, movement related effects still persist even after perfect realignment. Movement related effects can be divided into those that are a function of the position of the object into the frame of reference of the scanner and those that are due to movement in the previous scans. This second component depends on the history of excitation experienced by spins in a small volume and consequent differences in local saturation. The spin excitation history thus will itself be a function of previous positions, suggesting an auto-regression-moving average model for the effects of previous displacements on the current signal. In order to solve the above issue, the method proposed [17] takes the following form. (i) Estimate the movement parameters by comparing each scan in the time-series to a reference scan. This is made by expressing the difference between the scan in question and the reference scan as the sum of all partial derivatives of the image, with respect to each movement component, times the amount of each component. (ii) Realign the time series using the parameter estimates above. (iii) Adjust the values of each voxel by

removing any component that is correlated with a function of movement estimates, obtained at the time of the current scan and the previous scan. The above method was implemented and now constitutes a widely used software package, called Statistical Parametric Mapping (SPM), for fMRI series alignment and analysis.

CHAPTER 2

METHODS

They consist of three straightforward alignment methods which may have a range of applicability broader than only fMRI or MRI. They are based on fiducial markers, eigenvectors of Inertia of the Neuro-Images, and rotation-translation matrices. To validate these three techniques, an automated procedure was developed that applies a known rigid body transformation to the Neuro-Images. This procedure allowed for evaluating the performance of the technique described earlier [1], its derivational techique and the three fiducial markers technique used previuosly [10]-[11]. The results of alignment of the three methods were then compared across imaging modalities (fMRI and MRI) and for high and low resolution. The idea was that if we knew in advance the rigid body transformation applied to the human brain during scanning, then we could judge whether or not the results that we get by alignment procedures are reliable.

2.1 The Simulation of Head Movement in Neuro-Images

We are given three angles: Pitch (Θ rotation about the X axis of the head coordinate system), Roll (ϕ rotation about the Y axis of the head coordinate system), and Yaw (ψ rotation about the Z axis of the coordinate system) and three coordinates (Δx, Δy and Δz translations from the center of gravity of the brain). A rigid body transformation **R** was computed as the sum of a generic rotation **rot** about the axes

of a coordinate system passing through the center of gravity of the brain, and a generic translation **t**. A right hand coordinate system was used.

Generic Rotation matrix:

$$\mathbf{rot} = \begin{vmatrix} r_{xx} & r_{xy} & r_{xz} \\ r_{yx} & r_{yy} & r_{yz} \\ r_{zx} & r_{zy} & r_{zz} \end{vmatrix} \tag{1}$$

Rotation about the X axis:

$$Pitch = \begin{vmatrix} 1 & 0 & 0 \\ 0 & \cos \Theta & -\sin \Theta \\ 0 & \sin \Theta & \cos \Theta \end{vmatrix} \tag{2}$$

Rotation about the Y axis:

$$Roll = \begin{vmatrix} \cos \phi & 0 & -\sin \phi \\ 0 & 1 & 0 \\ \sin \phi & 0 & \cos \phi \end{vmatrix} \tag{3}$$

Rotation about the Z axis:

$$Yaw = \begin{vmatrix} \cos \psi & -\sin \psi & 0 \\ \sin \psi & \cos \psi & 0 \\ 0 & 0 & 1 \end{vmatrix} \tag{4}$$

Generic Translation

$$\mathbf{t} = \begin{vmatrix} t_x \\ \\ t_y \\ \\ t_z \end{vmatrix} \qquad\qquad (5)$$

The result were computed in the form $\mathbf{R} = \mathbf{rot}*\mathbf{P} + \mathbf{t}$, where $\mathbf{rot}$ was the matrix resulting from the multiplication between Pitch Roll and Yaw matrices, and $\mathbf{P}$ is the generic voxel. For the i-th voxel, which associated intensity was above a threshold T, the coordinates of the center of gravity were found as:

$$X_{Cog} = [\ \Sigma_i\, x_i\, /\, N\ ] \qquad\qquad (6)$$

$$Y_{Cog} = [\ \Sigma_i\, y_i\, /\, N\ ] \qquad\qquad (7)$$

$$Z_{Cog} = [\ \Sigma_i\, z_i\, /\, N\ ] \qquad\qquad (8)$$

Where N was the Number of pixels above the threshold T and where $x_i\, y_i$ and z_i are respectively the x, y and z coordinates of the pixels above the threshold T. The Neuro-Images are an assembly of voxels each of which is labeled by 3 indexes (x, y and z) which assume integer value. The application of the transformation $\mathbf{R}$ to the voxel coordinates produces new voxel coordinates that are floating-point values. The Neuro-Images were re-sliced by interpolation. The effect of the interpolation is explained as follows. When we apply the transformation $\mathbf{R}$ to the 3D Neuro-Image, we apply a matrix multiplication and a matrix addiction to the values of the coordinates of the voxels (which are originally expressed by integer values). Such matrices operations produce new voxel coordinates (floating-point values) that we

want to use to display the new transformed Neuro-Image (see Fig. 1). When the floating-point values are truncated into integers, some voxels may be lost because they have the same integer part. Therefore holes may be created in the transformed Neuro-Image. To solve this problem the following was done. (i) A priori interpolation of the Neuro-Image was performed. This was made by computing for each given pixel, the new pixel intensity as the average value of the 3 by 3 by 3 pixels' cube containing that given pixel at its center. (ii) The transformation **R** was applied to the grid of voxels and the values of the new coordinates of the voxels (truncated floating-point values) were obtained. (iii) The holes of the new grid were filled with the voxels interpolated at step (i).
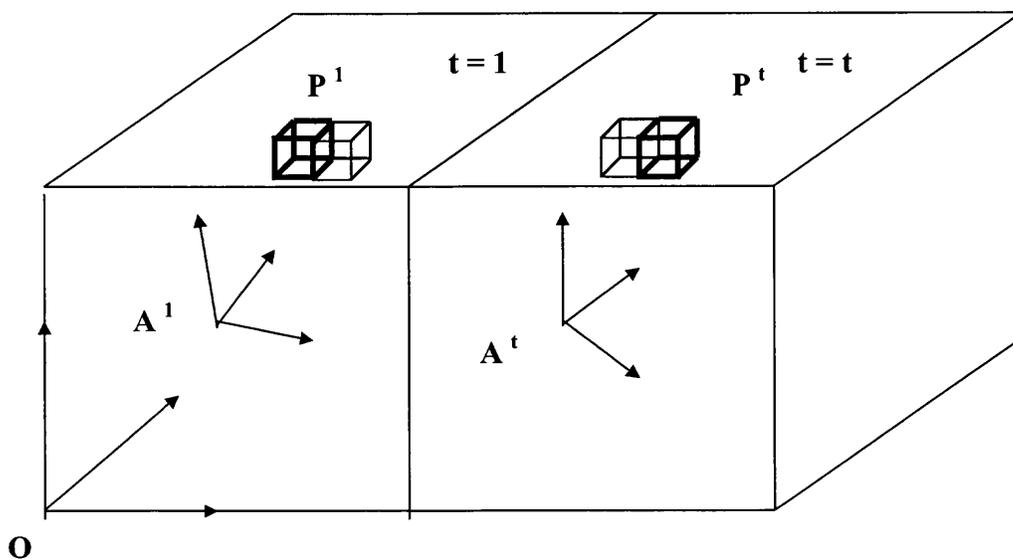
Figure 1. Neuro-Image Transformation.

Figure 1. Above figure illustrates the idea of how the new voxels are moved within the fMRI volume. At time t = 1 because of the given position of the brain, the

voxels assume an initial configuration P^1. At time t = t, applying the transformation **R**, the voxels assume a new position P^t within the volume. The new position is identified by floating-point numbers, which were truncated into integers. At time t = t, one or more voxels may assume the same position. Therefore there will be holes in the new Neuro-image (the Neuro-image resulting from the application of the transformation **R**). To fill the holes we have used interpolation.

2.1.1 Computation of Pitch, Roll, Yaw and the Coordinates of the Origin of the Head Coordinate System.

The six parameters that describe the six degrees of freedom of the head in the space are the three angles pitch, yaw and roll and the three coordinates x y and z of the origin of the head coordinate system. In the case of the principal axes transformation method and its variant, the coordinates of the origin can be found easily by finding the center of mass of the Neuro-Image. In the case three fiducial markers technique, three points located respectively at the left and right ears and the nose can find the coordinates of the origin easily, since the method requires that the origin be at the midpoint between the ear's markers.

To determine the three angles pitch, yaw and roll, a more complicate procedure must be applied. Either given eigenvectors of the symmetric inertia matrix or given the unit vectors of the head coordinate system, for both reference Neuro-Image and test Neuro-Image, it is possible to compute above three angles. The yaw angle (rotation about the Z-axis) can be found by the angle between the x-axes and the y-axes (on the XY plane) of the coordinate system of the reference Neuro-Image and

the coordinate system of the test Neuro-Image. Particularly, since both eigenvectors and unit vectors are orthogonal, the angles between x-axes and the angle between y-axes were averaged. Similarly, the pitch and roll angles (respectively the rotations about X- axis and Y-axis) can be found by averaging the angles between y and z-axes, and x and z-axes respectively. Once the three angles and the three coordinates of the origin are found, then the rigid body transformation can be computed and applied to the test Neuro-Image.

2.2 The Implementation of the Principal Axes Transformation Method.

Given a reference Neuro-Image and a test Neuro-Image the method described in literature [1] computes the rigid body transformation to be applied to the test image, to align it to the reference image, in the following way. First of all the symmetric Inertia matrix of the Neuro-Image is computed. Such matrix express the meaning of a variance-covariance matrix computed for the Neuro-Image on the basis of the coordinates of the brain voxels, assuming that each voxel has unitary mass. The entries of the symmetric inertia matrix were found as:

$$I_{xx} = [\ \Sigma_i\ (\ x_i - \alpha\ )^2\ /\ N\ ] \qquad (9)$$

$$I_{yy} = [\ \Sigma_i\ (\ y_i - \beta\ )^2\ /\ N\ ] \qquad (10)$$

$$I_{zz} = [\ \Sigma_i\ (\ z_i - \gamma\ )^2\ /\ N\ ] \qquad (11)$$

$$I_{xy} = I_{yx} = [\ \Sigma_i\ (\ x_i - \alpha\ ) * (\ y_i - \beta\ ) / N\ ] \qquad (12)$$

$$I_{yz} = I_{zy} = [\ \Sigma_i\ (\ y_i - \beta\ ) * (\ z_i - \gamma\ ) / N\ ] \qquad (13)$$

$$I_{zx} = I_{xz} = [\ \sum_i (\ z_i - \gamma\ ) * (\ x_i - \alpha\ )^2 / N\ ] \qquad (14)$$

Where N was the Number of pixels above the threshold T. Where α, β and γ where the average values of respectively x y and z coordinates of the pixels found above the threshold T. The use of the threshold T aimed to roughly segment the Neuro-Image and therefore to eliminate the pixels' intensities outside the brain which may be incorporate signal relevant to thermal noise. The eigenvectors of such a matrix are computed and they express the meaning of the directions into the space along which the maximal variation of the pixel coordinates distribution is identified. Such directions (eigenvectors) can be interpreted as the coordinate system of the head. Having the directions of the coordinate systems of both reference image and test image, the angles between eigenvectors (pitch yaw and roll) can be computed, and the transformation to be applied to the test image can be retrieved. Such transformation is applied with respect to the center of mass of the head. To implement this technique the following steps were carried out. First of all the technique was tested for a two dimensional problem. Given a MRI Neuro-Image in 2D, artificial image was fabricated applying a rotation-translation to the original image. The Inertia matrix in 2D and the relative eigenvectors were computed for both images. The angle between eigenvectors was used to compute the 2D rotation-translation matrix that describes the 2D rigid body transformation. Applying such criterion, the angle of rotation in the plane was safely and correctly retrieved. The transformation could be applied to the original image to check if the technique described earlier [1] was effective. Figure 2 shows the original image (a), the image after a 10-degrees rotation has been applied about the axis perpendicular to the

image, through the center of mass (b), and the image after the rigid body transformation, retrieved from eigenvectors has been applied (c). Images (b) and (c) were the same and therefore I had the confirmation that the method reported in Ref. [1] was effective in 2 Dimensions for a 256 x 256 Neuro-Image.

(a)   (b)   (c)
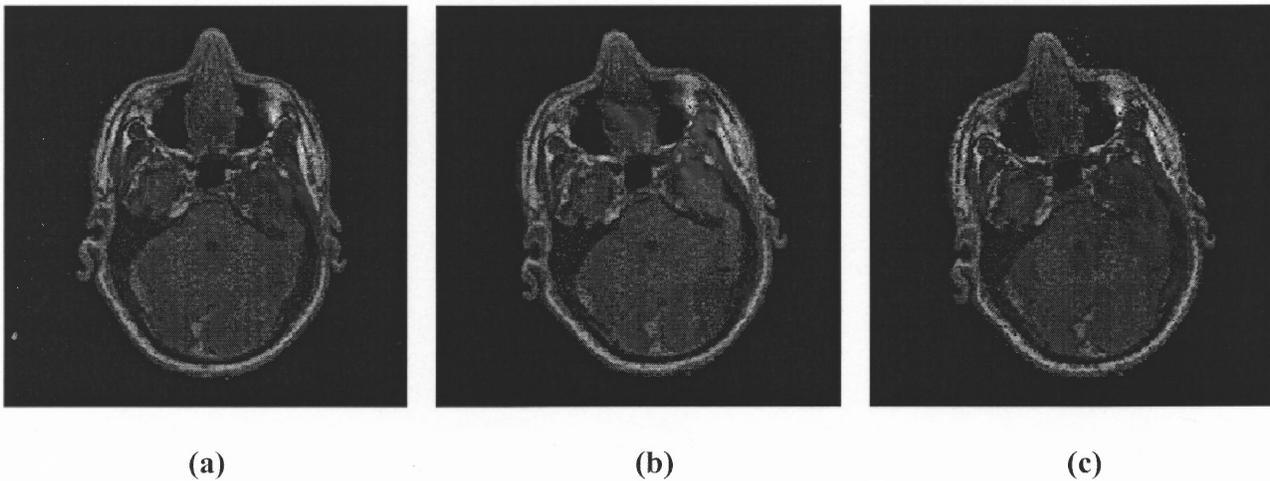
Figure 2. Test of the Principal Axis Transformation Method.

Figure 2. An original Neuro-Image (a). An artificial Neuro-Image produced applying a 10-degrees rotation about the axis perpendicular to the image and passing through the center of mass (b). The image obtained applying the rigid body transformation retrieved by the eigenvectors of Inertia (c). The method described in literature [1] was tested satisfactorily for a 2D Neuro-Image.

To solve the problem in 3 Dimensions, the Jacobi-Algorithm [15] was developed to compute the eigenvectors of the 3 x 3 Inertia Matrix. The algorithm, given a symmetric matrix, diagonalize it, and computes the eigenvalues (which are the non-zero entries of the diagonal matrix) and the corresponding eigenvectors.

The algorithm performs the computation of the eigenvectors on the basis of the Jacobi rotation matrix that identifies a right-hand coordinate system or a left-hand coordinate system. To test the performance of the algorithm, the results we compared to those of Matlab and Splus5. Such comparison, suggested that the algorithm computes correctly both eigenvalues and eigenvectors. Table I shows the results of the computation of the eigenvectors for Matlab, Splus5 and my algorithm. Note that the values are almost the same.

Inertia Matrix before diagonalization		
532.05	*8.75*	*-4.29*
8.75	*329.79*	*-49.17*
-4.29	*-49.17*	*407.59*
eigenvalues of Jacobi algorithm		
532.79	*305.83*	*430.81*
eigenvectors of Jacobi algorithm		
0.996	*-0.026*	*0.078*
0.056	*0.9*	*-0.478*
-0.056	*0.433*	*0.874*
eigenvalues of Matlab		
532.79	*305.83*	*430.8*
eigenvectors of Matlab		
0.996	*-0.026*	*0.074*
0.056	*0.9005*	*-0.431*
-0.056	*0.434*	*0.899*
eigenvalues of Splus5		
532.78	*305.83*	*430.8*
eigenvectors of Splus5		
0.996	*-0.026*	*0.075*
0.056	*0.9051*	*-0.431*
-0.056	*0.434*	*0.899*

Table I. Inertia Eigenvalues and Eigenvectors for a given Neuro-Image.

Table I. The table shows from the top to the bottom the Inertia before diagonalization, the eigenvalues and the eigenvectors for Jacobi algorithm, Matlab and Splus5 respectively. The eigenvectors express the meaning of the direction along which the voxel's coordinates have maximum variation. Matlab, Splus5 and our algorithm computed the eigenvectors of a right hand coordinate system. The values resulted to be the same suggesting that our algorithm performed correctly.

2.3 The Implementation of the Variant to the Principal Axes Transformation Method.

What made our Principal Axes Transformation Method implementation weak was the use of threshold T to select the pixels above a given arbitrary intensity. As said above, the use of the threshold T has the meaning of a rough segmentation that aims to select only those pixels relevant to the brain for the computation of the inertia matrix. This implied that changing the value of the threshold, the alignment performance of the method changed accordingly. This is because the numerical values of the symmetric inertia matrix are computed on the basis of the coordinates of the pixels above the arbitrary threshold. To make the method more robust, then a technique that cancels out the pixels outside the brain without the need of an arbitrary threshold, should have been tried. To cancel out the pixels outside the brain we then used the intensity of the pixels themselves. We weighted the pixels' coordinates for the computation of the inertia matrix with the pixel intensity. We conducted a set of experiments on the basis of such methodology. The formula used are reported as follows:

$$X_{Cog} = [\; \Sigma_i \; x_i * f(p_i) / \Sigma_i \; f(p_i) \;] \qquad (15)$$

$$Y_{Cog} = [\; \Sigma_i \; y_i * f(p_i) / \Sigma_i \; f(p_i) \;] \qquad (16)$$

$$Z_{Cog} = [\; \Sigma_i \; z_i * f(p_i) / \Sigma_i \; f(p_i) \;] \qquad (17)$$

$$I_{xx} = [\; \Sigma_i \; (x_i - \alpha)^2 * f(p_i) / \Sigma_i \; f(p_i) \;] \qquad (18)$$

$$I_{yy} = [\; \Sigma_i \; (y_i - \beta)^2 * f(p_i) / \Sigma_i \; f(p_i) \;] \qquad (19)$$

$$I_{zz} = [\; \Sigma_i \; (z_i - \gamma)^2 * f(p_i) / \Sigma_i \; f(p_i) \;] \qquad (20)$$

$$I_{xy} = I_{yx} = [\; \Sigma_i \; (x_i - \alpha) * (y_i - \beta) * f(p_i) / \Sigma_i \; f(p_i) \;] \qquad (21)$$

$$I_{yz} = I_{zy} = [\; \Sigma_i \; (y_i - \beta) * (z_i - \gamma) * f(p_i) / \Sigma_i \; f(p_i) \;] \qquad (22)$$

$$I_{zx} = I_{xz} = [\; \Sigma_i \; (z_i - \gamma) * (x_i - \alpha)^2 * f(p_i) / \Sigma_i \; f(p_i) \;] \qquad (23)$$

Where N was the Number of pixels above the threshold T. Where α, β and γ where the average values of respectively x y and z coordinates of the pixels found above the threshold T. Where $f(p_i)$ was the value of the ith pixel intensity. Outside the brain however the pixel intensity is only due to thermal noise and to introduce such component in the computation of the inertia matrix may be faulty because the thermal noise may affect the computation of the inertia and consequently the computation of the eigenvectors. We then decided that, prior to the computation of the values of the inertia matrix by the pixels' intensity, we also should have threshold the Neuro-Image with T such to remove the thermal noise from the computation of the symmetric inertia matrix. Therefore the implementation of the

variant to the principal axes transformation method aimed to develop an alignment method based on the pixel's intensity. This might have served to compare the performances of the present technique to the performance of the original principal axes transformation method (not dependent on pixel's intensity).

2.4 The Three Fiducial Markers based Technique

To use fiducial markers to align Neuro-Images may seem to be primitive and obsolete given that a lot of effort has been spent in last few years to develop fully automated techniques. However, we present this method for two reasons. The first reason is that the method itself is innovative because it is based only on three fiducial markers, which we demonstrate are enough to cover the six degree of freedom in a 3D Neuro-Image. The algorithm used to build up the head coordinate system has been developed for previous research [10]-[11] and now we have generalized to MRI and fMRI. The second reason is that we believe this methodology is the ideal and most straightforward alignment technique if the resolution of the Neuro-Images is high enough. In this regard we will explore its performances in following sections of the present paper.

2.4.1 Construction of the Head Coordinate System.

Given three reference points, the first at the location of the right ear, the second at the location of the left ear and the third at the nose, a right hand head coordinate system can be built. The mathematical method used in order to build the coordinate system is as follows. The equation of plane (i) passing through the three points is computed, and the midpoint between ears is stored as the origin of the head coordinate system. The equation of a second plane (ii) is found by the constraint

that it must be perpendicular to plane (i) and passing through the origin of the coordinate system and the nose. The third plane (iii) is found by the constraint that it must be perpendicular to the planes (i) and (ii) and must pass through the origin of the coordinate system. The constraints ensure a univocal solution of the problem. Each plane is therefore found by three constraints. However, the coefficients of the mathematical equation of the plane in a three dimensional space are four. The likely assumption that the human brain cannot make rotations bigger than 90-degrees imposes that one of the coefficients of the planes (ii) and (iii) is equal to one. This translates in the fact that the axis of the coordinate system cannot make an angle bigger than 90-degrees with the axis of the fixed coordinate system. Therefore the problem of finding a plane can be solved with three constraints even though there are four unknown coefficients. Applying this method, the unit vectors of the head coordinate system were computed both for reference Neuro-Images and test Neuro-Images.

2.5 Validation of the Methods.

To validate the three techniques, artificial Neuro-Images were created. They were derived applying a rigid body transformation to an original image. The idea is that if we knew a prior the transformation applied to the Neuro-Image, we could then evaluate the reliability of retrieval of the head motion in the Neuro-Images and therefore we could evaluate the performance of the techniques.

2.6 Software Implementations

To carry out this work, two software systems were built: EIGEN and ALIGN. These systems were developed using three software environments: Matlab, Open

GL and ANSI C. Matlab was used in order to build GUIs (Graphical User Interfaces). OpenGL was used to for Interactive Graphics to display the MRI and fMRI data. ANSI C was used to write the routines that performed the mathematical computations necessary to apply the two techniques. The software systems were implemented on a SGI Onyx 2 machine and are currently in use.

Figure 3 shows the GUI of the EIGEN software system. Figure 3a shows the GUI used to fabricate artificial Neuro-Images to which a 3D rigid body transformation is applied. The "Display Scan" button activates a program that displays the Neuro-Image by an OpenGL application. The GUI controls the X Y and Z resolution of the three dimensional Image. The Open GL application displays three composite 2D views (Plane sections, Sagittal Sections and Coronal Sections) that can be sliced interactively by the keyboard. The GUI allows the user to input the values of the pitch, roll and yaw angles and the values of the three coordinates that are needed in order to apply the rigid body transformation to the Neuro-Image. There is also a "Display info" button that allows the user to get information on how to set up the X Y and Z resolution of the three dimensional Neuro-Image. Once the options of the GUI are set, then the "Comp Matrix" button computes pitch, roll and yaw matrix. The "Roto-trasl" button applies the transformation and finally the "ReDisplay Scan" button redisplays the transformed Neuro-Image. This last button controls another Open GL application that can be driven interactively by the use of the keyboard. Figure 3b shows the GUI used to estimate the rigid body transformation applied by the GUI of Figure 3a. The "Display Scan" button performs as above. The "Eigenvectors" button activates a program that computes

the symmetric inertia matrix of the Neuro-Image and the relative eigenvectors on the basis of the principal axes transformation method. The "Eigenmass" button do the same with the simple difference that computes the symmetric inertia matrix and the relative eigenvectors on the basis of the variant to the principal axes transformation method. The "AlignScan" button applies the transformation to the test image. The "Reference Scan" is specified in the GUI as a name of a file containing the eigenvectors of the Reference Neuro-Image. Once the computation is performed, the "ReDisplay" button, displays the scan that has been aligned to the reference Neuro-Image.
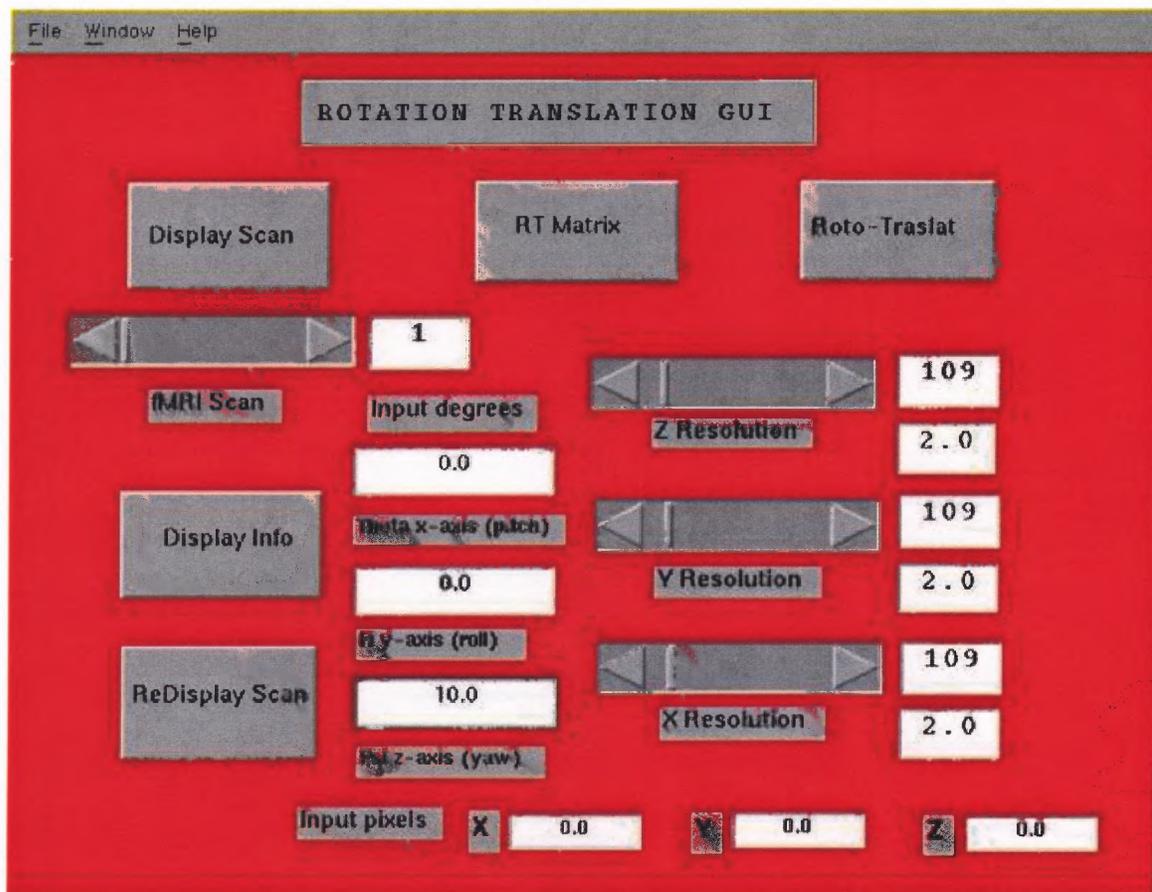
Figure 3a. The GUI used by EIGEN to Fabricate Artificial Neuro-Images.
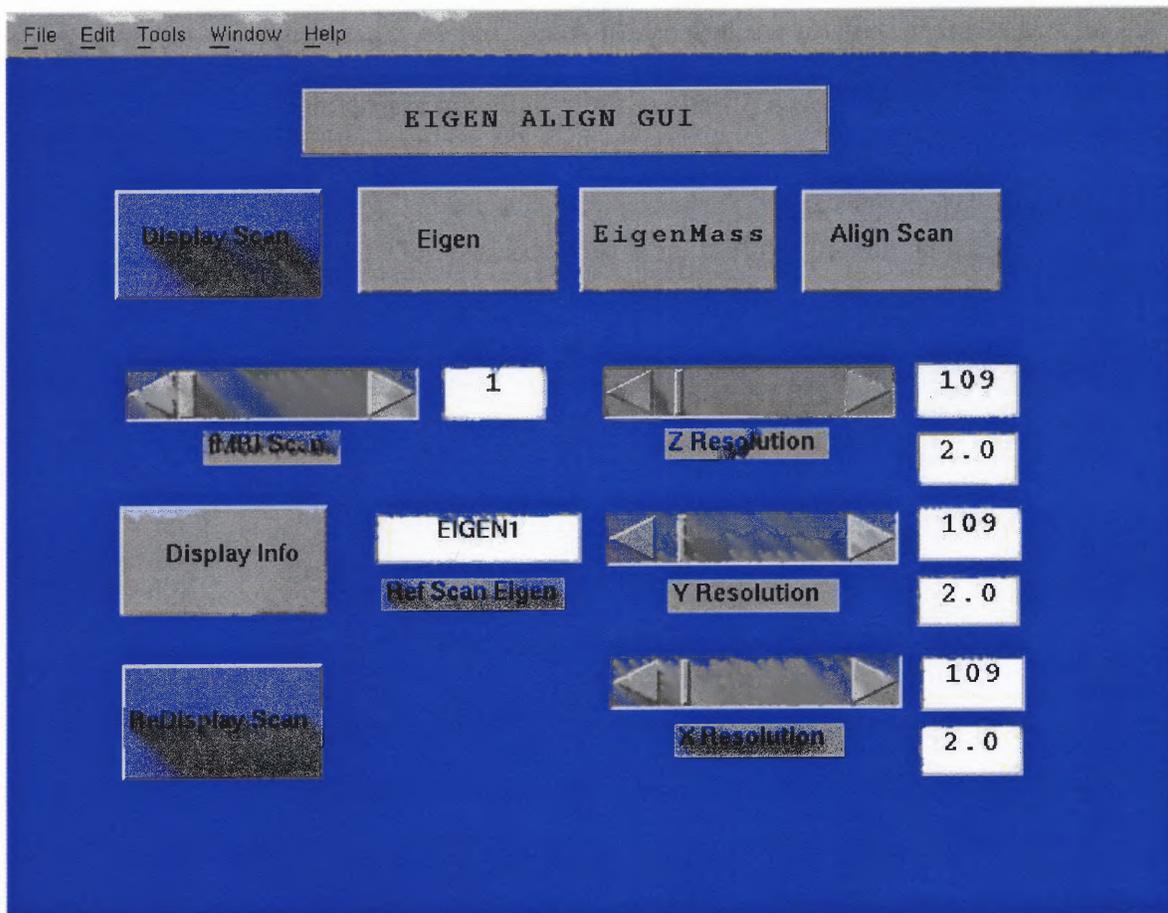
Figure 3b. The GUI used by EIGEN to Align Neuro-Images.

Fig. 3. The two GUIs of the EIGEN system. Fig. 3a shows the GUI used to create the artificial Neuro-Images. Fig. 3b shows the GUI used to implement the principal axes transformation method and its variant for the alignment of two Neuro-Images.

Figure 4 shows the GUI of the ALIGN software system. Figure 4a shows the GUI used to fabricate artificial Neuro-Images. The computations performed by this GUI are the same as those of the EIGEN software system except for the "Choose Markers" button that allows the user to choose, interactively, by an Open GL

application, the three points into the Neuro-Image. The aim of this GUI as those illustrated in Figure 3a is that of applying a transformation to the Neuro-Image. Except that in this case the Neuro-Image will contain also the three points on the basis of which the head coordinate system and the unit vectors will be computed.

Figure 4b shows the GUI used to estimate the rigid body transformation applied by the GUI of Figure 4a. The "Display Scan" button performs as above. The "Comp. Versors" button activates a program that computes the unit vectors of the head coordinate system of the Neuro-Image. The "AlignScan" button applies the transformation to the test Neuro-Image.
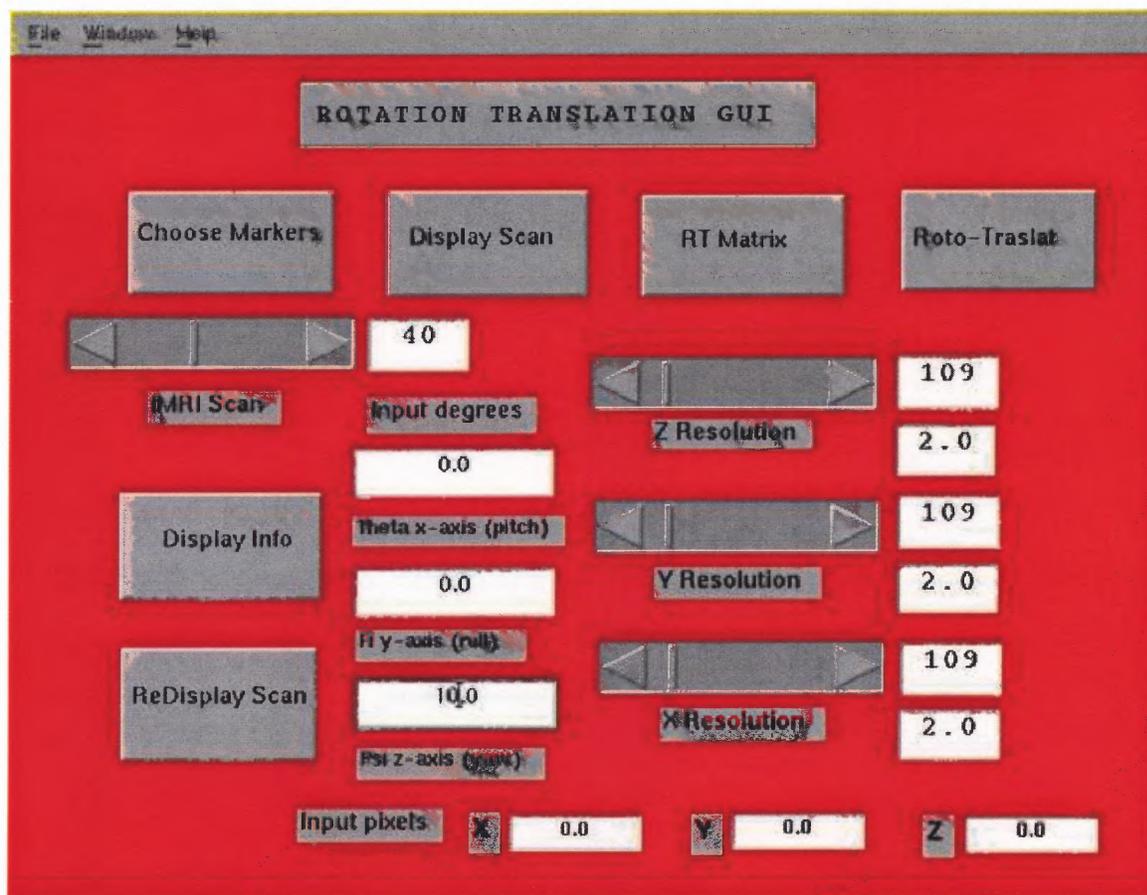
Figure 4a. The GUI used by ALIGN to Fabricate Artificial Neuro-Images.

The "Reference Scan" is specified in the GUI as a name of a file containing the unit vectors of the Reference Neuro-Image. Once the computation is performed, the "ReDisplay" button, redisplays the scan that has been aligned to the reference Neuro-Image.
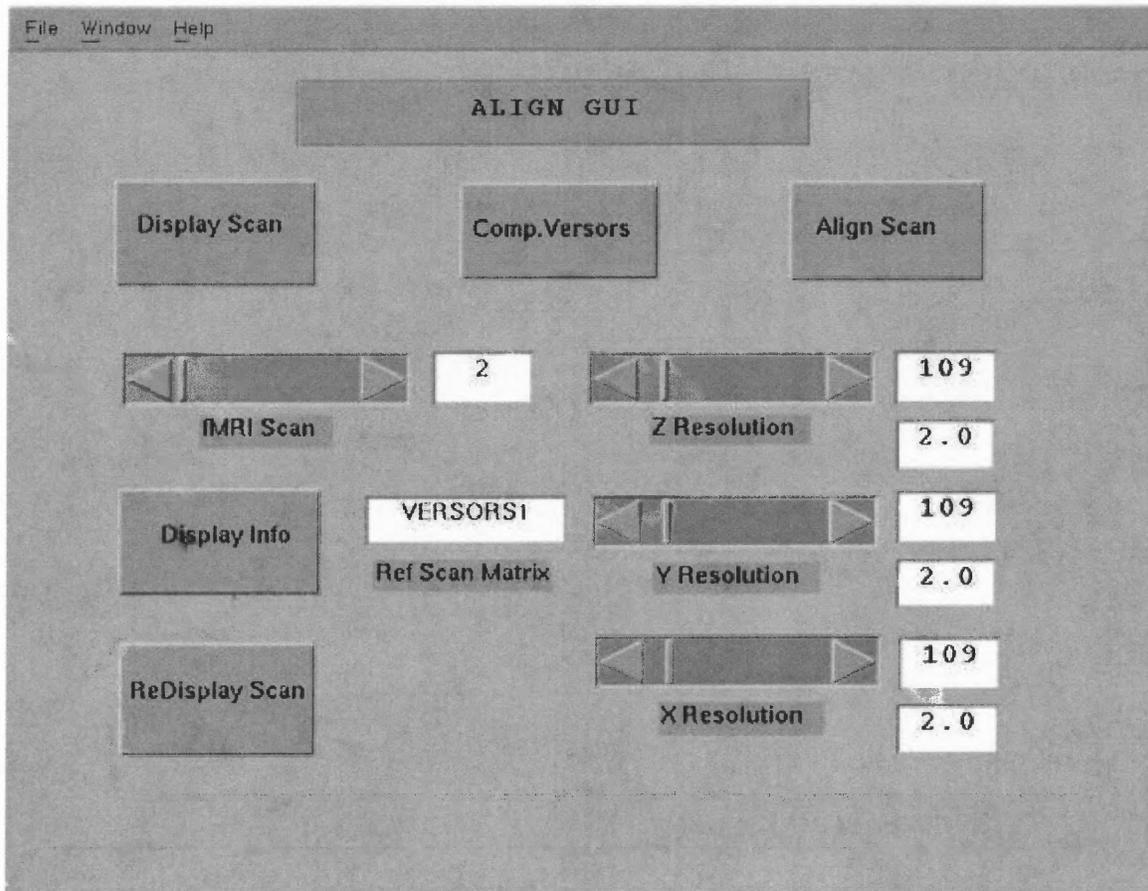

Figure 4b. The GUI used by ALIGN to Align Neuro-Images.

Fig. 4. The two GUIs of the ALIGN system. Fig. 4a shows the GUI used to create into the Neuro-Images the three points on the basis of which our technique makes the computation of the head coordinate system. Fig. 4b shows the GUI used

to align the two Neuro-Images, by the computation of the angles between unit

vectors of the head coordinate systems.

CHAPTER 3

RESULTS

The two software systems (EIGEN and ALIGN) implemented the three techniques called EIGEN, MASS and ALIGN which are respectively the principal axes transformation method, its variant based on pixels' intensity, and the three fiducial markers technique. In this section of the paper we presents their results and the evaluation of their performances for the three sets of experiments performed respectively with a fMRI Neuro-Image, with a low resolution MRI Neuro-Image and with a high resolution MRI Neuro-Image.

3.1 fMRI Neuro-Images

The three techniques (EIGEN, ALIGN and MASS) were tested with a 64 x 64 x 28 fMRI Neuro-Image. Good alignment results were obtained by the method reported in literature [1] (the principal axes transformation method), but poor results were obtained by both the fiducial markers technique and the variation of the principal axes transformation method. The experiments were conducted to see how (within a large movement range [-10°; 10°]) pitch, jaw and roll were estimated individually. Furthermore, experiments were conducted in the same movement range, to see how pitch, jaw and roll were estimated when they were imposed concurrently to the artificial Neuro-Image. Figure 5a shows the results of the method described in literature [1] (EIGEN). Figure 5b shows the results of the variant based on pixels' intensity (MASS). Figure 5c shows the results of the fiducial markers method (ALIGN).
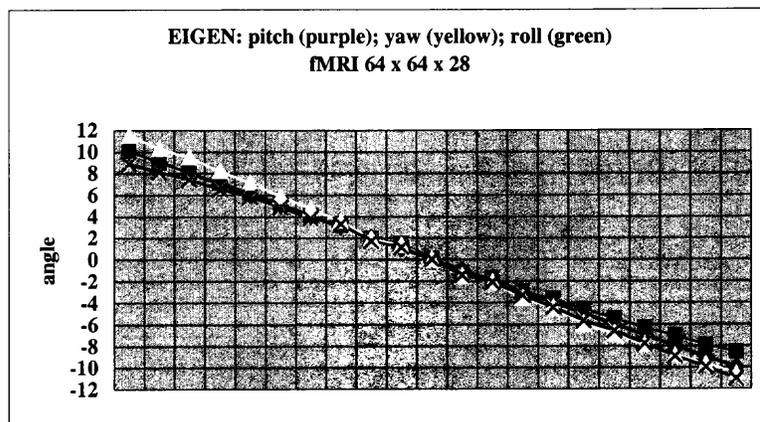
Figure 5a. Performance of EIGEN with a 64 x 64 x 28 fMRI volume
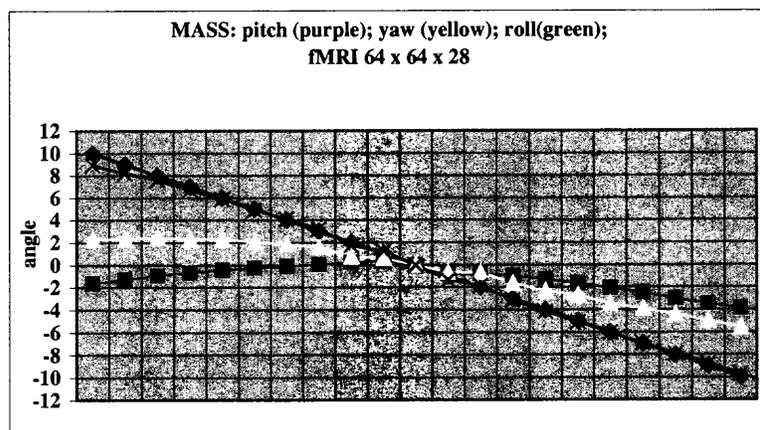
Figure 5b. Performance of MASS with a 64 x 64 x 28 fMRI volume
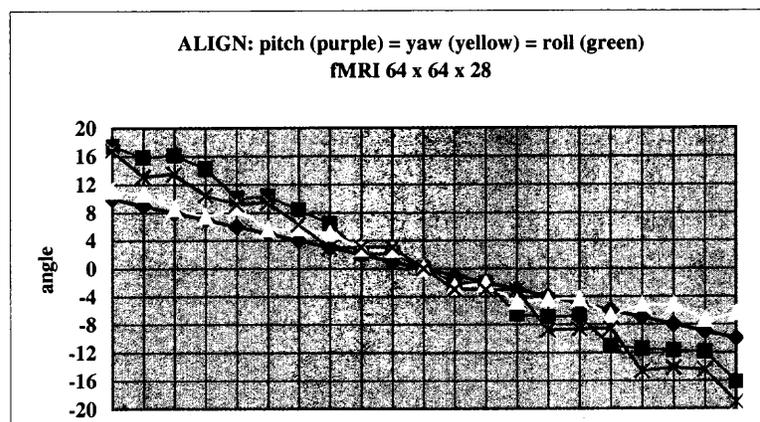
Figure 5c. Performance of ALIGN with a 64 x 64 x 28 fMRI volume

Fig. 5. Performance of EIGEN, MASS and ALIGN techniques in estimating

pitch, yaw and roll angles for a 64 x 64 x 28 fMRI volume. The blue line connects
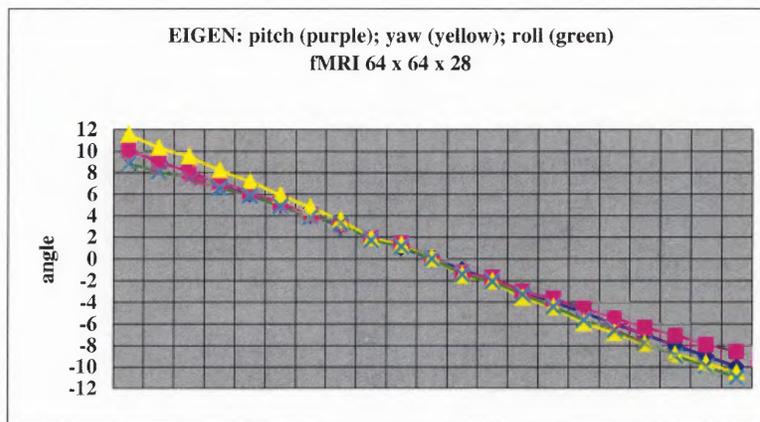
**Figure 5a. Performance of EIGEN with a 64 x 64 x 28 fMRI volume**
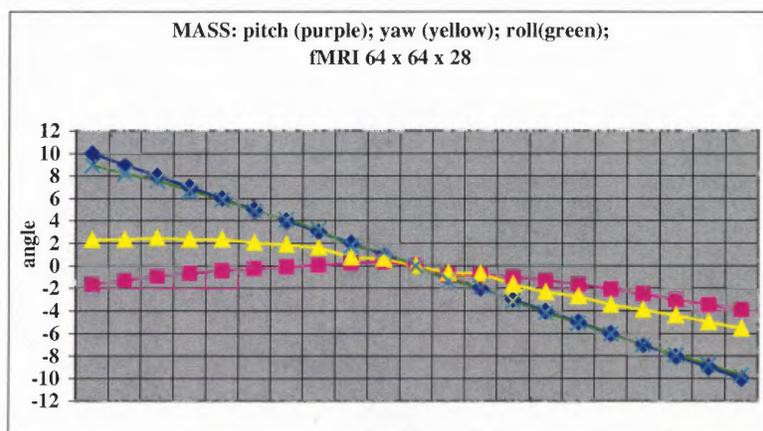
Figure 5b. Performance of MASS with a 64 x 64 x 28 fMRI volume
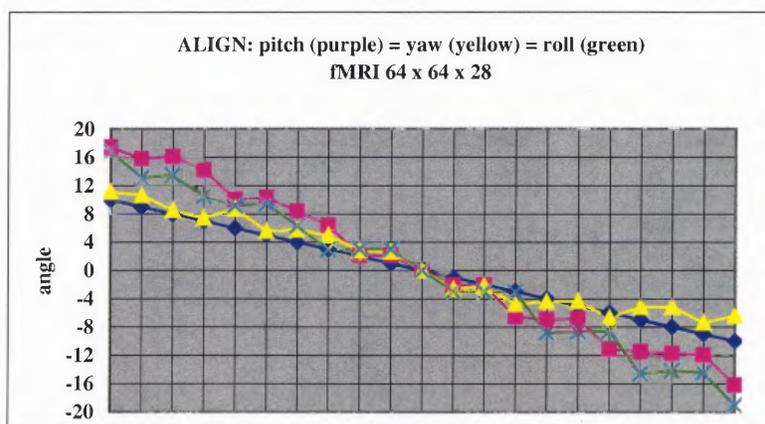

Figure 5c. Performance of ALIGN with a 64 x 64 x 28 fMRI volume

Fig. 5. Performance of EIGEN, MASS and ALIGN techniques in estimating

pitch, yaw and roll angles for a 64 x 64 x 28 fMRI volume. The blue line connects

the values of the angle that were used to fabricate the artificial Neuro-Images, and represents the ideal performance of the techniques. All of the pitch, yaw and roll had the same value. Once the rigid body transformation is applied to the Neuro-Image, the performance of the three techniques EIGEN MASS and ALIGN is expressed by the purple (pitch), yellow (yaw) and green (roll) lines. Such lines did approximate satisfactorily the desired performance (blue line) in the case of EIGEN (a), while did not in the case of MASS (b) and ALIGN (c).

In all of the three figures the results are presented as follows. The blue line represents the expected performance of the technique, while the purple yellow and green lines represent respectively the estimated pitch, yaw and roll. These results show in the large movement range ([-10°; 10°]) that when the three rotations, pitch yaw and roll were imposed concurrently to the artificial Neuro-Image, the performances of two techniques (MASS and ALIGN) were poor, while the performance of the EIGEN technique was satisfactory. However ALIGN performed better than MASS.

Good performances were obtained by MASS and ALIGN techniques when they were asked to estimate the yaw angle alone. This last angle is the rotation about the Z-axis, which is perpendicular to the XY plane (a grid of 64 x 64 brain voxels). The X and Y directions were the major resolution directions. The results are shown in Figure 6a and Figure 6b respectively for MASS and ALIGN.
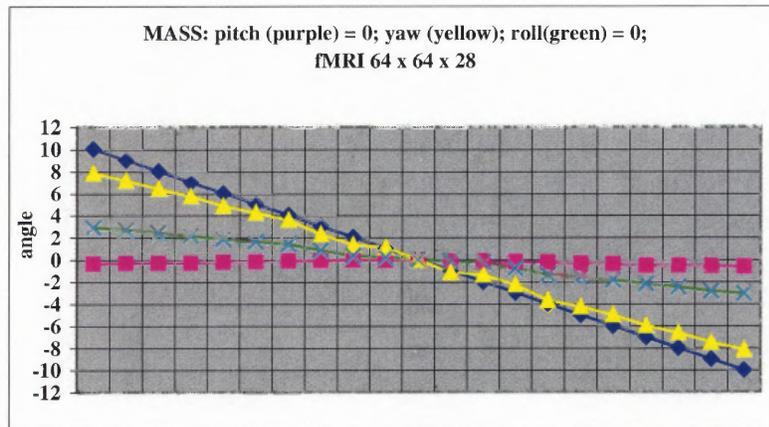
Figure 6a. Performance of MASS with a 64 x 64 x 28 fMRI volume in the estimation of the yaw angle.
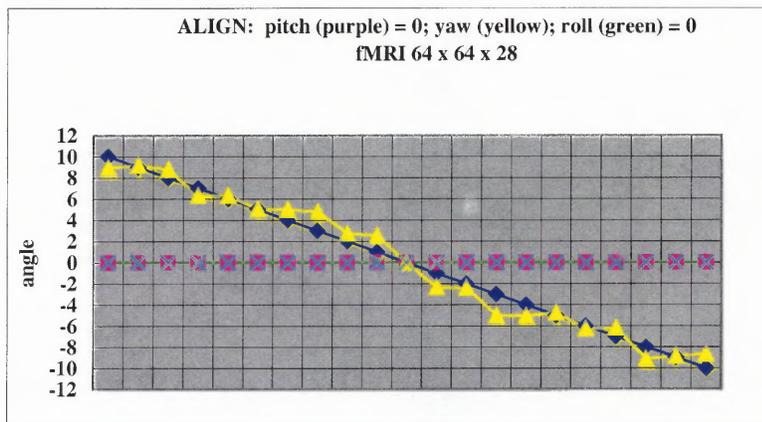
Figure 6b. Performance of ALIGN with a 64 x 64 x 28 fMRI volume in the estimation of the yaw angle.

Fig. 6. Performance of MASS (a) and ALIGN (b) techniques in the estimation of the yaw angle for a 64 x 64 x 28 fMRI volume. This picture shows the best results that were obtained for the experiments done on the 64 x 64 x28 fMRI volume. The yellow line (yaw) approximated satisfactorily the desired (ideal) performance of the system while the estimation of the other two angles (pitch and roll) was almost zero for MASS (a) and zero for ALIGN (b).

The yellow line (estimation of yaw angle) approximates satisfactorily the blue line (ideal performance of the system), while the purple and green lines are close to zero in the case of MASS and zero in the case of ALIGN. This last result is consistent with the fact that pitch and roll angles imposed to the artificial Neuro-Images were both zero. Such results were interpreted as follow. As said in the previous section of the paper, the test Neuro-Image is fabricated artificially. To fabricate the artificial Neuro-Image, we need to do interpolation. The result of the interpolation is that some pixels' intensities (those relevant to the hole created in the Neuro-Image) are altered. Being dependent on pixel intensity, the performance of MASS technique is therefore affected also by the interpolation. The fact that the best results were obtained for MASS when the yaw angle was imposed alone to the artificial Neuro-Image, are consistent with its dependence on the interpolation. This is because we found that when a rotation about the Z-axis is imposed, the number of holes created, and so the number of pixels for which the intensity is altered, is smaller than that number obtained when the rotation about the Y-axis is imposed. However, when a rotation about the X-axis is imposed to the artificial Neuro-Image, we found that the number of holes created is even less than those created by the yaw rotation. The latter suggests that MASS may be dependent also on the axial sampling resolution.

As far as the performance of ALIGN is concerned, it is dependent on the choice of three fiducial markers. The fiducial markers have in our system (ALIGN) the size of one pixel. The technique is dependent on the axial resolution of the Neuro-Images. When a rotation about the Z-axis is imposed to the artificial Neuro-Image,

the markers are moved along the grid of major resolution (64 x 64). This cause the error of alignment to be dependent on the major resolution and therefore it is less than it could be when the other two possible rotations (about X or Y axes) are imposed. This explains why ALIGN technique expressed its best performance when only the yaw angle was imposed to the artificial Neuro-Image.

3.2 MRI Low Resolution Neuro-Images

Tests were performed of the three techniques with a 64 x 64 x 28 MRI volume obtained by sub-sampling of the original Neuro-Image. Also in these experiments we investigated (within a large movement range $[-10°; 10°]$) pitch, jaw and roll, were estimated individually. Furthermore, experiments were conducted in the same movement range, to see how pitch, jaw and roll were estimated when they were imposed concurrently to the artificial Neuro-Image. The aim of these sets of experiments was that of investigating if we could confirm also for MRI the findings obtained earlier for fMRI Neuro-Images. These tests give information on how the techniques perform for different imaging modalities (fMRI and. MRI) when the axial resolution is the same. We were expecting to confirm the reliability of EIGEN technique, to confirm that the performance of MASS technique is affected by interpolation, and to confirm that the performance of ALIGN technique is strongly depending on the axial resolution. All of the findings were confirmed by these sets of experiments. When the pitch, yaw and roll were imposed concurrently to the artificial Neuro-Image we had the following results. The performance of the EIGEN technique was confirmed satisfactory and even slightly better than the one

obtained with a 64 x 64 x 28 fMRI volume. We think this slight increase in performance is attributable to the fact that the MRI shape of the head is such to have less degree of symmetry with the respect to the principal axes, whereas in fMRI given that only functional data is collected, the shape of the head has an higher degree of symmetry with respect to the principal axes. The latter imply that the eigenvectors solutions may not be unique [1] for fMRI Neuro-Images.

The performance of MASS did not change much with respect to that obtained with a 64 x 64 x 28 fMRI volume. There was a little increase in the performance of the estimation of the negative yaw angle. This small improvement in the performance can be attributable to the previously mentioned fact that MASS technique bases the computation of the eigenvectors on the pixels' intensity. MRI has more pixels' intensity variability than fMRI both in range because of the different physical phenomenon underling the two imaging techniques, and in spatial distribution because of the less degree of symmetry of the head in MRI with respect to fMRI. Therefore we propose that the larger pixel's intensity variability was used by MASS method to embed in the eigenvectors more information relative to the position of the head into the volume. The performance of ALIGN was the same as that obtained with a 64 x 64 x 28 fMRI volume. This was as expected since ALIGN technique precision is dependent on the size of the fiducial markers. Given that the resolution of MRI was the same as that of the experiments conducted with the fMRI volume, then the performances in MRI were not different from those obtained in fMRI. Figure 7 shows the graphs relative to above results. Figure 7a. shows the performance of EIGEN, while Figures 7b and 7c show those of MASS

and ALIGN respectively. Overall EIGEN produced the best performances, followed by ALIGN and then MASS. This confirmed the results obtained with the 64 x 64 x 28 fMRI volume. Good results were obtained when MASS and ALIGN techniques were tested for the estimation of the yaw angle alone. Figures 8a and 8b show such results respectively for MASS and ALIGN. As it can be seen by Figures 8a and 8b both MASS and ALIGN performed correctly. There was then an improvement of the results obtained by MASS with respect to the experiments conducted with the fMRI volume. The fact can be explained in the following terms. The MRI volume contains more pixels' intensity variability due to the fact that MRI modality scans the anatomy of the head thus producing more variability in both range and spatial distribution, whereas fMRI scans only the functional activation thus has less pixels' intensity variations. Therefore the variability in the MRI pixels' intensity translates in information collected by the eigenvectors about the position of the head in the volume. The performance shown in Figure 8a is however the best of MASS for this set of experiments. As said previously thermal noise and interpolation affects negatively MASS technique. As for the interpolation the case of the estimation of the yaw angle is the case in which the number of pixels' for which the intensity is altered is less with respect to the other case of a rotation about the Y-axis. In the 64 x 64 grid, X and Y were the directions of major resolution.
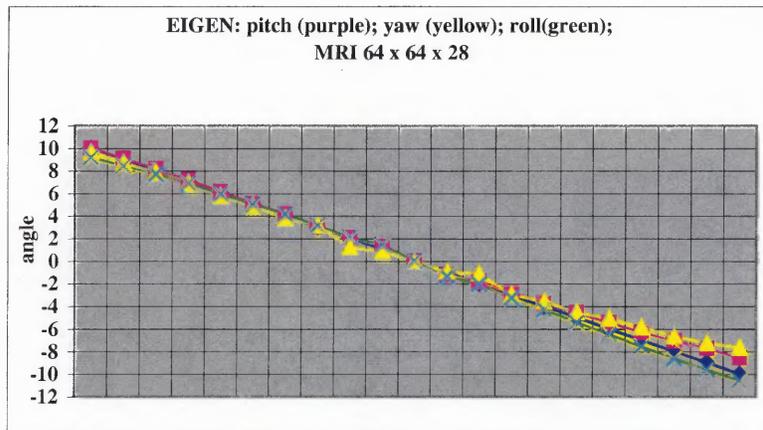
Figure 7a. Performance of EIGEN with a 64 x 64 x 28 MRI volume
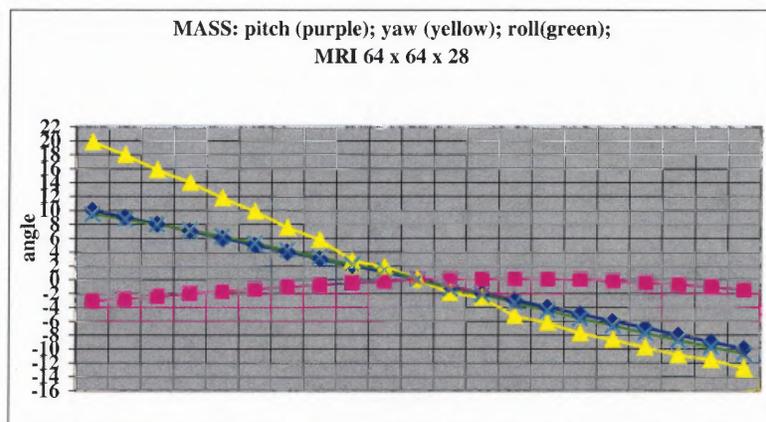
Figure 7b. Performance of MASS with a 64 x 64 x 28 MRI volume
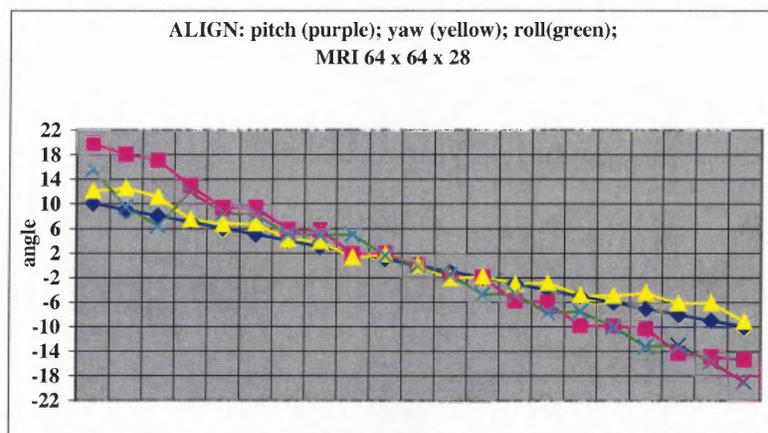
Figure 7c. Performance of ALIGN with a 64 x 64 x 28 MRI volume

Fig. 7. Performance of EIGEN, MASS and ALIGN techniques in estimating pitch, yaw and roll angles for a 64 x 64 x 28 MRI volume. The performances of the three techniques are the purple (pitch), yellow (yaw) and green (roll) lines. Such lines did approximate satisfactorily the desired performance (blue line) in the case of EIGEN (a), while did not in the case of MASS (b) and ALIGN (c). The results were similar to those reported for the fMRI volume with the same sampling resolution. The difference with respect to the experiments conducted with fMRI is that there was a slight improvement in the estimation of the negative yaw angle by the MASS technique. In general however ALIGN performed better than MASS.
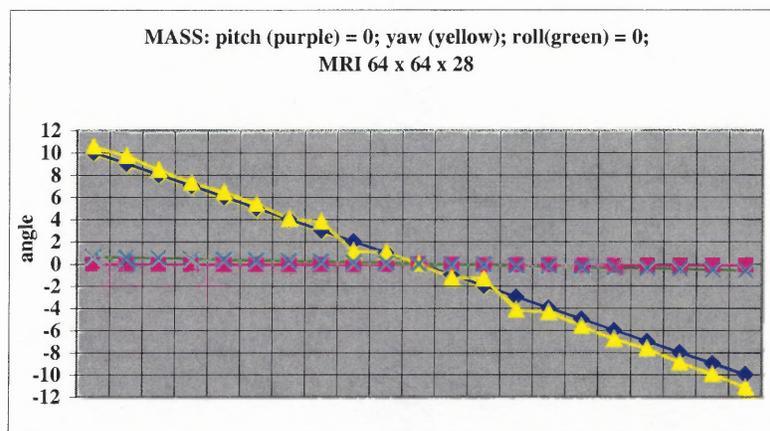
Figure 8a. Performance of MASS with a 64 x 64 x 28 MRI volume in the estimation of the yaw angle.
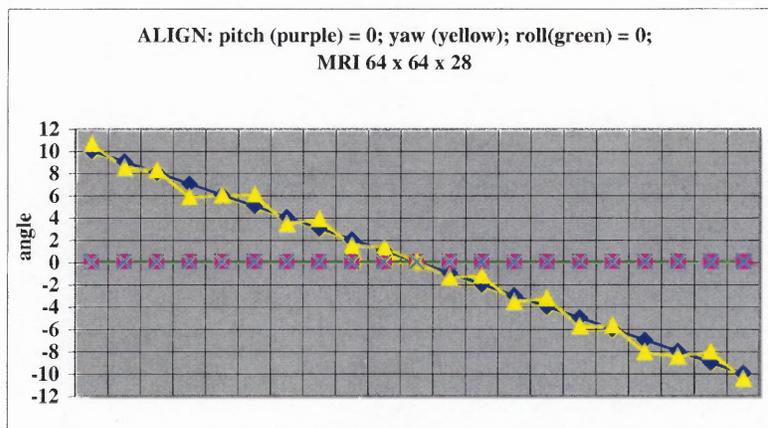
Figure 8b. Performance of ALIGN with a 64 x 64 x 28 MRI volume in the estimation of the yaw angle.

Fig. 8. Performance of MASS (a) and ALIGN (b) techniques in the estimation of the yaw angle for a 64 x 64 x 28 MRI volume. This picture shows the best results that were obtained for the experiments for which the pitch, yaw and roll angle are imposed singularly to the artificial Neuro-Image. The yellow line (yaw) approximated satisfactorily the desired (ideal) performance of the system while the estimation of the other two angles (pitch and roll) was zero both for MASS (a) and ALIGN (b).

3.3 MRI High Resolution Neuro-Images

Tests were performed of the three techniques with a 109 x 109 x 109 MRI volume. The aim of these sets of experiments was that of confirming also for high resolution MRI the findings obtained earlier for fMRI Neuro-Images. We were expecting to confirm the reliability of the EIGEN technique, to confirm that the performance of the MASS technique is affected by the interpolation, and to investigate possible improvements in the performance of the ALIGN technique. All of the findings were confirmed by these sets of experiments. The resolution of the MRI volume was such high that ALIGN technique improved and performed better than EIGEN technique. All of the pitch, yaw and roll angles were satisfactorily estimated individually by ALIGN technique in the large movement range ([-10°; 10°]). Figure 9 shows the results obtained by the estimation of the yaw angle for ALIGN technique. As it can be seen from the picture, the degree of fit of the yellow line to the blue (ideal) line improved largely with respect to the results presented in Figure 6b. The estimation of pitch, yaw and roll angles individually of EIGEN technique was generally slightly worse than that performed by ALIGN technique. The results obtained by the estimation of the yaw angle by EIGEN are reported in Figure 10, respectively for the 64 x 64 x 28 fMRI volume (a) and the 109 x 109 x 109 MRI volume (b). As it can be seen in the figure, there was a small error in the estimation of pitch and roll, given that only the yaw angle was applied to the Neuro-Image.

ALIGN: pitch (purple) = 0; yaw (yellow); roll (green) = 0
MRI 109 x 109 x 109
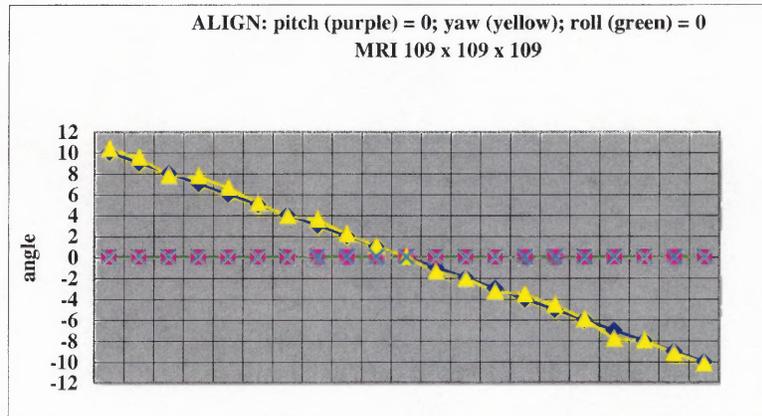
Figure 9. Performance of ALIGN with a 109 x 109 x 109 MRI volume in the estimation of the yaw angle.

Fig 9. Estimation of the yaw angle of ALIGN technique for a high resolution 109 x 109 x 109 MRI volume. The degree of fit of the yellow (estimated) line to the blue line (ideal) improved largely with respect to that presented in Figure 6a.

EIGEN: pitch (purple) = 0; yaw (yellow); roll (green) = 0
fMRI 64 x 64 x 28
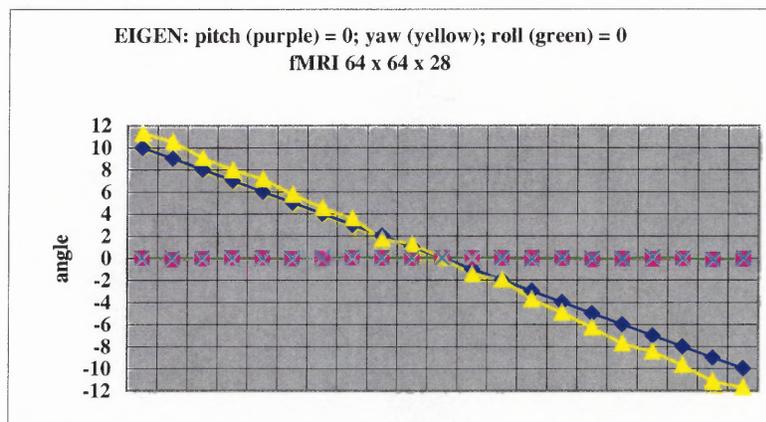
Figure 10a. Performance of EIGEN with a 64 x 64 x 28 fMRI volume in the estimation of the yaw angle.
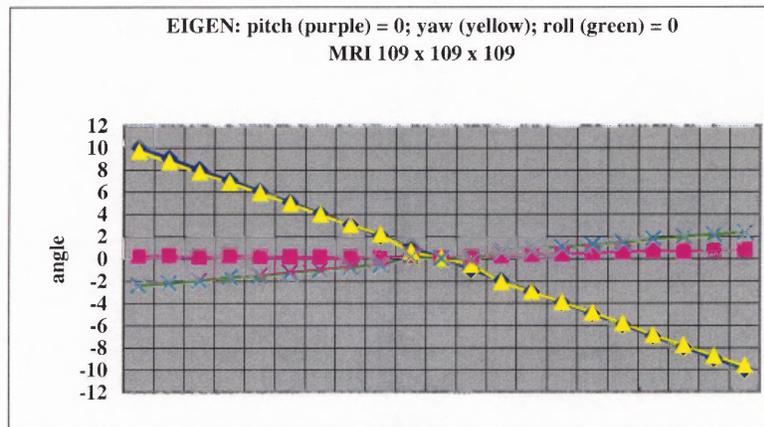
Figure 10b. Performance of EIGEN with a 109 x 109 x 109 MRI volume in the estimation of the yaw angle.

Fig. 10. Estimation of the yaw angle of the EIGEN technique for a fMRI volume (a), and a high resolution MRI volume (b). The degree of fit of the yellow line (estimated yaw) to the blue line (ideal yaw) increased with the increase of the resolution, while the degree of fit of the purple (estimated pitch) and the green (estimated roll) lines decreased with the increase of resolution. As far as the estimation of the yaw angle is concerned, the behavior of EIGEN technique was the same as that shown by ALIGN technique. For the estimation of the other two angles, ALIGN technique was more reliable with the increase of resolution.

When the two techniques were tested with the estimation of the three angles (pitch, yaw and roll) concurrently, it was found out that ALIGN system performed better than EIGEN technique. Figure 11 shows the performance of both techniques for the 109 x 109 x 109 MRI volume. The estimated lines (purple, yellow and

green), as illustrated by Figure 11, were closer to the ideal line (blue) in the case of the ALIGN technique.
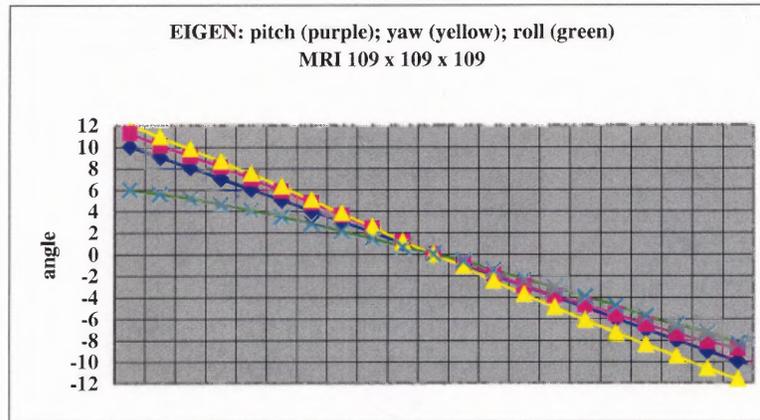
Figure 11a. Performance of EIGEN with a 109 x 109 x 109 MRI volume.
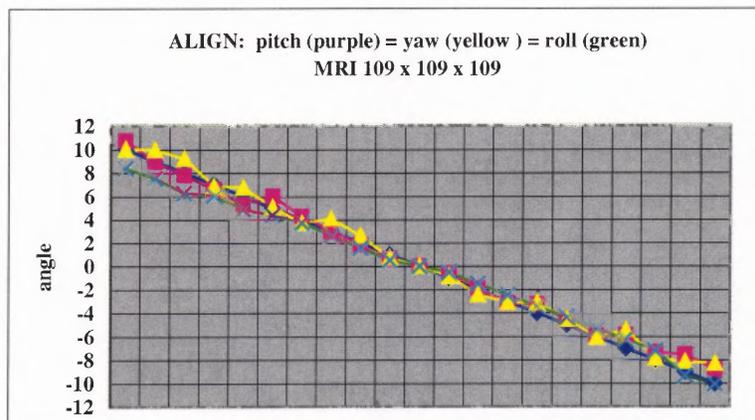
Figure 11b. Performance of ALIGN with a 109 x 109 x 109 MRI volume.

Fig. 11. Performances of EIGEN and ALIGN systems in estimating pitch, yaw and roll angles for a 109 x 109 x 109 MRI volume. The performances of EIGEN and ALIGN techniques is expressed by the purple (pitch), yellow (yaw) and green (roll) lines. The performance of the EIGEN technique (a) was worse than that of the ALIGN technique (b).

As far as MASS technique is concerned, the results we obtained were generally poor. As said previously MASS technique is dependent on the pixel intensity. Since the interpolation alters the original pixel's intensity, the overall performance is affected and the so the results were poor. We report in Figure 12 the performance obtained for the estimation of the yaw angle alone. As it can be seen in the picture there is degradation in the performances with respect to those obtained with the 64 x 64 x 28 fMRI and MRI volumes. The reason of this behavior can be attributable to the fact that the increase of resolution produces a larger number of pixels' intensities altered by the interpolation.
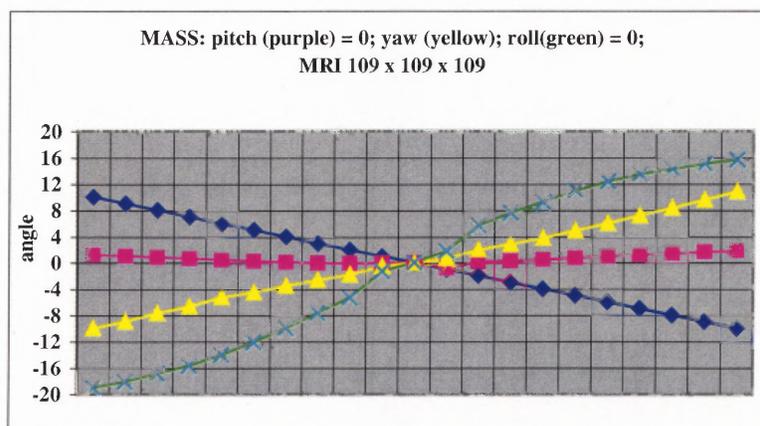
Figure 12. Performance of MASS with a 109 x 109 x 109 MRI volume in the estimation of the yaw angle.

Fig. 12. Performance of MASS in the estimation of the yaw angle for a 109 x 109 x 109 MRI volume. The results were poor and can be attributable to the large number of pixels' intensities altered by the interpolation. These results were worse than those reported in Figure 6a and Figure 8a respectively for the estimation of the yaw

angle for a 64 x 64 x 28 fMRI and MRI volumes. The number of pixels' intensities altered by interpolation is larger for a 109 x 109 x 109 MRI volume.

3.4 Comparison Between the Three Techniques

The results presented in the previous sections revealed the following findings. EIGEN technique was the most reliable for low resolution Neuro-Images both fMRI and MRI with a sensible increase in precision in MRI with respect to fMRI because MRI provides Neuro-Images with smaller degree of symmetry along the principal axes than fMRI. Therefore in MRI, the eigenvector problem has more likely unique solution. This is in agreement with what reported earlier [1]. MASS and ALIGN techniques were less reliable for low resolution Neuro-Images both fMRI and MRI. However, ALIGN performed generally better than MASS. There are three findings relative to the two techniques. MASS was confirmed to be dependent on the thermal noise, on the sampling axial resolution, on the pixels' intensity and also on the interpolation. The latter is because the interpolation we have used altered the original pixels' intensity for some of the voxels. ALIGN was confirmed to be dependent on the sampling axial resolution. This is because its precision is strictly dependent on the choice of the three fiducial markers which size of each is the same axial resolution of the Neuro-Image. MASS performed better for low resolution MRI than for fMRI because of the larger variability in pixels' intensity both in range and in position. This is because a larger variability in the pixel's intensity translates in more information embedded into the eigenvectors about the position of the head into the volume.

When the experiments were extended to high resolution MRI above findings were confirmed and it was found that ALIGN outperformed EIGEN. This reveals that for sufficiently high axial resolution our fiducial makers technique is more reliable than the principal axes transformation method. This is because the precision of ALIGN is inversely proportional to the sampling axial resolution.

A summary of the results obtained by the three techniques is illustrated in Tables II and III. For each of the experiments, the degree of fit was computed of the purple, yellow and green lines (performances of the systems) with the blue line or zero line. The degree of fit was expressed as the root mean square of the sum of the squared differences between the desired values and the obtained performance. Table II shows such degree of fit for each of the three techniques (EIGEN, MASS and ALIGN) and for each of the three volumes used in our experiments (fMRI, and low resolution and high resolution MRI), for the large movement range [-10°; 10°]. Table III shows the same for the small movement range [-3°; 3°].

As said previously we aimed to compare EIGEN and ALIGN to a technique depending on the pixels' intensity. We have then developed MASS as a variant of EIGEN. While EIGEN uses a threshold to roughly segment the brain MASS uses the pixels' intensity. Outside the brain however the pixels' intensity is either zero or it is thermal noise. To eliminate the thermal noise we have done a set of experiments in which a threshold could be applied to the Neuro-Image before the computation of the inertia matrix. The experiments were developed to see if the elimination of the thermal noise would have produced improvements in the techniques' performances. We did the experiments applying simultaneously pitch,

yaw and roll to the Neuro-Image. Tables II and III show the resulting degree of fit

for these tests (dof (t.b.i)). We found that the results did not change confirming hat

the MASS techniques' performance was poor. Therefore we can report that MASS

technique is affected negatively by axial sampling resolution and interpolation.

To compare the performances of the three techniques within the same modality and

the same axial sampling resolution we have computed a t-value on the basis of the

average degree of fit for each experiment. The t-value was computed with the

following formula:

$$t = X_1 - X_2 / S_p \qquad (24)$$

Where X_1 and X_2 are the average values of the degree of fit for the techniques

(EIGEN, MASS and ALIGN) within the same sampling resolution, and S_p is the

pooled variance of the degree of fit. We report in tables IV and V the resulting t-

values. The meaning of the t-value is that of expressing in a pair wise comparison

which of two techniques works better for a given modality (fMRI or MRI) and a

given sampling resolution (64 x 64 x 28 or 109 x 109 x 109). Tables IV and V

show the mean degree of fit (mean dof) for each technique together with the t-value

of the couple of techniques. While a positive t-value express that the technique on

the left column of the tables works worse than the technique on the right, a negative

t-value express the opposite meaning (i.e. that the technique on the left column of

the tables is overall performing better than the technique of the right column).

Large Movements Range [-10 deg; 10deg]								
fMRI 64x64x28			**MRI 64 x 64 x 28**			**MRI 109x109x109**		
EIGEN	*pitch*	*yaw=0*	*roll=0*	*pitch*	*yaw=0*	*roll=0*	*pitch*	*yaw=0*	*roll=0*
dof	*1.01*	*0.54*	*0.97*	*1.48*	*0.22*	*0.52*	*4.48*	*0.8*	*0.45*
	pitch=0	*yaw=0*	*roll*	*pitch=0*	*yaw=0*	*roll*	*pitch=0*	*yaw=0*	*roll*
dof	*0.87*	*0.66*	*2.27*	*0.51*	*1.34*	*1.18*	*1.21*	*6.53*	*0.95*
	pitch=0	*yaw*	*roll=0*	*pitch=0*	*yaw*	*roll=0*	*pitch=0*	*yaw*	*roll=0*
dof	*0.3*	*5.26*	*0.29*	*0.023*	*1.74*	*1.14*	*1.74*	*1.04*	*6.8*
	pitch	*yaw*	*roll*	*pitch*	*yaw*	*roll*	*pitch*	*yaw*	*roll*
dof	*2.26*	*3.93*	*2.84*	*2.38*	*3.83*	*1.95*	*3.25*	*5.77*	*8.1*
fMRI 64x64x28			**MRI 64 x 64 x 28**			**MRI 109x109x109**		
MASS	*pitch*	*yaw=0*	*roll=0*	*pitch*	*yaw=0*	*roll=0*	*pitch*	*yaw=0*	*roll=0*
dof	*23.78*	*0.5*	*1.12*	*31.53*	*1.2*	*0.316*	*29.51*	*2.36*	*10.75*
	pitch=0	*yaw=0*	*roll*	*pitch=0*	*yaw=0*	*roll*	*pitch=0*	*yaw=0*	*roll*
dof	*2.26*	*8.88*	*7.72*	*4.1*	*18.56*	*1.02*	*1.73*	*35.45*	*60.24*
	pitch=0	*yaw*	*roll=0*	*pitch=0*	*yaw*	*roll=0*	*pitch=0*	*yaw*	*roll=0*
dof	*1.59*	*5.56*	*8.4*	*0.38*	*3.03*	*1.71*	*4.02*	*55.59*	*55.33*
	pitch	*yaw*	*roll*	*pitch*	*yaw*	*roll*	*pitch*	*yaw*	*roll*
dof	*25.14*	*16.24*	*1.61*	*31.18*	*20.45*	*2.14*	*32.27*	*94.93*	*93.57*
	pitch	*yaw*	*roll*	*pitch*	*yaw*	*roll*	*pitch*	*yaw*	*roll*
dof (t.b.i)	*22.13*	*17.41*	*4.26*	*33.2*	*15.32*	*2.21*	*39.73*	*46.49*	*157.38*
fMRI 64x64x28			**MRI 64 x 64 x 28**			**MRI 109x109x109**		
ALIGN	*pitch*	*yaw=0*	*roll=0*	*pitch*	*yaw=0*	*roll=0*	*pitch*	*yaw=0*	*roll=0*
dof	*26.28*	*1.29*	*0.14*	*18.79*	*1.44*	*7.57*	*2.43*	*1.11*	*2.42*
	pitch=0	*yaw=0*	*roll*	*pitch=0*	*yaw=0*	*roll*	*pitch=0*	*yaw=0*	*roll*
dof	*9.46*	*3.34*	*19.2*	*7.6*	*4.72*	*20.07*	*2.42*	*3.43*	*2.51*
	pitch=0	*yaw*	*roll=0*	*pitch=0*	*yaw*	*roll=0*	*pitch=0*	*yaw*	*roll=0*
dof	*0*	*4.49*	*0*	*0*	*3.08*	*0*	*0*	*1.77*	*0*
	pitch	*yaw*	*roll*	*pitch*	*yaw*	*roll*	*pitch*	*yaw*	*roll*
dof	*20.67*	*7.47*	*20.09*	*20.3*	*7.35*	*17.94*	*2.94*	*3.48*	*3.82*

Table II. The Degree of fit of the Three Techniques for the Large Movement Range.

Table II. For each experiment, for each of the three techniques (EIGEN, MASS and ALIGN), and for each modality the table indicates, in the large movements range, the degree of fit (dof) of the performance of the technique to the ideal performance. The degree of fit was computed as the root mean square of the sum of the square differences between the expected value (ideal) and the performance.

Small Movements Range [-3 deg; 3deg]									
	fMRI 64x64x28			MRI 64 x 64 x 28			MRI 109x109x109		
EIGEN	pitch	yaw=0	roll=0	pitch	yaw=0	roll=0	pitch	yaw=0	roll=0
dof	0.85	0.22	0.1	1.36	0.173	0.089	1.07	0.164	0.124
	pitch=0	yaw=0	roll	pitch=0	yaw=0	roll	pitch=0	yaw=0	roll
dof	0.22	0.31	2.11	0.04	0.73	1.04	0.22	1.32	0.904
	pitch=0	yaw	roll=0	pitch=0	yaw	roll=0	pitch=0	yaw	roll=0
dof	0.02	1.12	0.14	0.08	1.49	0.22	0.511	0.626	1.46
	pitch	yaw	roll	pitch	yaw	roll	pitch	yaw	roll
dof	0.579	1.05	0.69	0.424	1.19	0.654	0.72	1.3	1.47
	fMRI 64x64x28			MRI 64 x 64 x 28			MRI 109x109x109		
MASS	pitch	yaw=0	roll=0	pitch	yaw=0	roll=0	pitch	yaw=0	roll=0
dof	3.96	0.122	0.164	6.11	0.7	0.07	5.69	0.96	3.63
	pitch=0	yaw=0	roll	pitch=0	yaw=0	roll	pitch=0	yaw=0	roll
dof	0.214	0.692	1.73	0.404	3.81	0.84	0.342	7.07	12.55
	pitch=0	yaw	roll=0	pitch=0	yaw	roll=0	pitch=0	yaw	roll=0
dof	0.361	1.37	1.2	0.16	1.78	0.336	0.88	10.12	13.53
	pitch	yaw	roll	pitch	yaw	roll	pitch	yaw	roll
dof	4.24	2.7	0.566	6.1	3.91	0.74	6.8	20.33	28.45
	pitch	yaw	roll	pitch	yaw	roll	pitch	yaw	roll
dof (t.b.i)	3.52	3.43	1.01	6.55	2.84	0.61	6.89	10.55	59.38
	fMRI 64x64x28			MRI 64 x 64 x 28			MRI 109x109x109		
ALIGN	pitch	yaw=0	roll=0	pitch	yaw=0	roll=0	pitch	yaw=0	roll=0
dof	9.48	0.72	0.07	4.44	0.76	4	0.59	0.56	1.28
	pitch=0	yaw=0	roll	pitch=0	yaw=0	roll	pitch=0	yaw=0	roll
dof	5.17	0.346	3.24	4.59	0.489	4.58	1.46	1.18	1.16
	pitch=0	yaw	roll=0	pitch=0	yaw	roll=0	pitch=0	yaw	roll=0
dof	0	3.45	0	0	1.47	0	0	0.78	0
	pitch	yaw	roll	pitch	yaw	roll	pitch	yaw	roll
dof	5.15	3.62	3.22	4.14	1.74	4.77	0.6	1.34	1.17

Table III. The Degree of fit of the Three Techniques for the Small Movement Range.

Table III. Performances of the three techniques (EIGEN, MASS and ALIGN) in the small movement range. The values of the degree of fit were obtained with the same criterion illustrated for table II, except that the square differences between the expected value (ideal) and the performance of the technique were computed within -3° and 3°.

Large Movements Range [-10 deg; 10 deg]		
	fMRI 64x64x28	
EIGEN	MASS	ALIGN
mean dof = 1.76	8.56	9.36
t-value	-0.01	-0.04
	fMRI 64x64x28	
MASS	EIGEN	ALIGN
mean dof = 8.56	1.76	9.36
t-value	0.01	-0.02
	fMRI 64x64x28	
ALIGN	EIGEN	MASS
mean dof = 9.36	1.76	8.56
t-value	0.04	0.02
	MRI 64 x 64 x 28	
EIGEN	MASS	ALIGN
mean dof = 1.35	9.63	9.07
t-value	-0.09	-0.176
	MRI 64 x 64 x 28	
MASS	EIGEN	ALIGN
mean dof = 9.63	1.35	9.07
t-value	0.09	0.205
	MRI 64 x 64 x 28	
ALIGN	EIGEN	MASS
mean dof = 9.07	1.35	9.63
t-value	0.09	-0.205
	MRI 109x109x109	
EIGEN	MASS	ALIGN
mean dof = 3.42	39.64	2.19
t-value	-0.01	0.296
	MRI 109x109x109	
MASS	EIGEN	ALIGN
mean dof = 39.64	3.42	2.19
t-value	0.01	0.302
	MRI 109x109x109	
ALIGN	EIGEN	MASS
mean dof = 2.19	3.42	39.64
t-value	-0.296	-0.302

Table IV. Pair Wise Comparison Between the Three Techniques in the Large Movement Range.

Table IV. The table reports the t-value for pair of techniques. The t-value was computed from Table II on the basis of the average degree of fit in the large movement range for the same sampling resolution in the same modality.

Re-examining

Small Movements Range [-3 deg; 3 deg]		
	fMRI 64x64x28	
EIGEN	MASS	ALIGN
mean dof = 0.617	1.44	2.87
t-value	-0.106	-0.02
	fMRI 64x64x28	
MASS	EIGEN	ALIGN
mean dof = 1.44	0.617	2.87
t-value	0.106	-0.08
	fMRI 64x64x28	
ALIGN	EIGEN	MASS
mean dof = 2.87	0.617	1.44
t-value	0.02	0.08
	MRI 64 x 64 x 28	
EIGEN	MASS	ALIGN
mean dof = 0.624	2.08	2.58
t-value	-0.13	-0.18
	MRI 64 x 64 x 28	
MASS	EIGEN	ALIGN
mean dof = 2.08	0.624	2.58
t-value	0.13	-0.283
	MRI 64 x 64 x 28	
ALIGN	EIGEN	MASS
mean dof = 2.58	0.624	2.08
t-value	0.18	0.283
	MRI 109x109x109	
EIGEN	MASS	ALIGN
mean dof = 0.82	9.19	0.84
t-value	-0.51	-0.032
	MRI 109x109x109	
MASS	EIGEN	ALIGN
mean dof = 9.19	0.82	0.84
t-value	0.51	0.546
	MRI 109x109x109	
ALIGN	EIGEN	MASS
mean dof = 0.84	0.82	9.19
t-value	0.032	-0.546

Table V. Pair Wise Comparison Between the Three Techniques in the Small Movement Range.

Table V. The table reports the t-value for pair of techniques. The t-value was computed from Table III on the basis of the average degree of fit in the small movement range for the same sampling resolution in the same modality.

From the two tables IV and V we can report the following general findings. EIGEN technique: (i) for small head movements it works better than MASS for fMRI (t-value = -0.106) and for both low resolution (64 x 64 x 28) and high resolution (109 x 109 x 109) MRI (respectively and t-value = -0.13 and t-value = -0.51). For small head movements it works better than ALIGN for fMRI (t-value = -0.02) and low resolution MRI (t-value = - 0.18). (ii) For any head movements in the range $-10°$ $10°$ it works better than MASS for fMRI (t-value = -0.01) and for both low resolution and high resolution MRI (respectively t-value = -0.09 and t-value = -0.01). For any head movement in the range $-10°$ $10°$ it works better than ALIGN for fMRI (t-value = -0.04) and low resolution MRI (t-value = - 0.176).

MASS technique: (i) for small head movements it works better than ALIGN for both fMRI and low resolution MRI (respectively t-value = -0.08 and t-value = - 0.283). (ii) For any head movements in the range $-10°$ $10°$ in low resolution fMRI it has similar behavior to that of ALIGN (t-value= -0.02).

ALIGN technique: (i) for small head movements in high resolution MRI it works better than MASS (t-value=-0.546) and the same as EIGEN (t-value = 0.032). (ii) For any head movements in the range $-10°$ $10°$ in high resolution MRI it works better than MASS (t-value=-0.302) and EIGEN (t-value = -0.296).

CHAPTER 4

DISCUSSION AND CONCLUSIONS

Image registration algorithms can be divided into main classes: those that depend on fiducial markers and those independent from any marker, so called computational methods. The general problem with the use of fiducial markers is that the technology must ensure that the markers are always imaged. Since the physics principles may vary from one imaging modality to another, the type of marker may vary too. However, excellent registration results have been obtained with either two [16], or four [4]-[5] fiducial markers in the case of registration of computed radiography (CR). In the automated algorithms, independent from fiducial or anatomical markers, the general factor limiting the overall accuracy is image noise [2]. In this paper we have developed and compared three algorithms that belong to the two mentioned classes, and we have used a straightforward method to test their performances. The method of testing is based on the following concept. If we knew in advance the rigid body transformation applied to a test Neuro-Image, we should then be able to evaluate better the performance of the head movement correction system. The techniques were based on the assumption that the human brain is subject to rigid motion during different scanning periods. This was also assumed by previous research [21]-[24]-[25].

As far as the determination of the head coordinate system it was proposed [24] a method that required the use of plexiglas plates attached to the head of the patient and it was proposed [12] to use two anatomical landmarks (the anterior and the

posterior commissure of the human brain) to build a Talairach-Tournoux coordinate system. It has been shown [21] that the position of the head into the scanning volume may be featured by a set of points. On the other hand, it was proposed here that in order to determine a head coordinate system with high degree of reliability, only three fiducial markers are needed. The method proposed here was shown to give accurate results for high resolution Neuro-Images. Earlier, such a method was used to co-registrate MEG with MRI [10]-[11], and now it has been generalized it to fMRI and MRI.

In addition to a research presented earlier [21], three simple methodologies were evaluated on the basis of the assumption that given a reference Neuro-Image, a unique coordinate transformation can be found. Such a transformation, if applied to the test Neuro-Image, makes it perfectly aligned to the Reference Neuro-Image. To find such coordinate transformation the inertia matrix of the Neuro-Images was computed as illustrated in literature [1] and with a variation based on pixels' intensity as proposed in this paper. A coordinate transformation was also found by three fiducial markers [10]-[11]. In the first technique presented in this paper, the eigenvectors of the inertia matrix of the Neuro-Image express the meaning of the directions of maximal variation of the pixels' coordinates and were used to identify the head coordinate system. Such a method was presented earlier [1] as the principal axes transformation method. In the second technique the eigenvectors of the inertia matrix were computed on the basis of the pixels' coordinated weighted by their intensity. In the third technique, the computation of the coordinate transformation was based on three reference points that were introduced in our

Neuro-Images. Based on these three fiducial markers, the head coordinate system was identified, and the transformation that uniquely described the rigid body movement of a test Neuro-Image, with respect to a reference Neuro-Image, was computed.

It was shown that the performance of the method based on fiducial markers is sensitive to the resolution of the Neuro-Images. Good results were obtained by the principal axes transformation method for both low resolution and high resolution Neuro-Images. The best results were obtained, for high resolution Neuro-Images, when the coordinate transformation was retrieved on the basis of the coordinate system identified by the three fiducial markers. The results obtained by the fiducial markers technique were satisfactory in the case of low resolution Neuro-Images only for the estimation of the yaw angle. The results improved largely when we aligned MRI volumes with 109 x 109 x 109 as axial sampling resolution. The worst results were obtained by the variant to the principal axes transformation method based on pixel intensity. We can report that its performances are dependent on pixels' intensity, thermal noise, axial sampling resolution and interpolation. The latter two variables act negatively decreasing further the performance of the technique, yet affected by thermal noise.

We can give the following conclusions. EIGEN technique: (i) It is independent from interpolation. (ii) It is dependent from modality (MRI or fMRI) because based the shape of the Neuro-Image. (iii) It is good for low resolution fMRI and both low resolution and high resolution MRI. (iv) It cannot be used to co-registrate MRI and fMRI because dependent from modality.

MASS technique: (i) It is dependent from interpolation and it is dependent from modality (MRI or fMRI) because dependent on the intensity of the pixels. (ii) It is dependent from the shape of the Neuro-Image because it is dependent from the intensity of the pixels. (iii) It is poor for both fMRI and low resolution and high resolution MRI because dependent from interpolation. (iv) It cannot be used to co-registrate MRI and fMRI because dependent from modality.

ALIGN technique: (i) It is independent from interpolation and independent from modality (MRI or fMRI) because based on fiducial markers. (ii) It is independent from the shape of the Neuro-Image because based on fiducial markers. (iii) It is poor for fMRI and low resolution MRI because its precision is based on the choice of fiducial markers which size is the same of the resolution. (iv) It can be used to co-registrate MRI and fMRI with a same resolution because independent from modality.

REFERENCES

[1]   Alpert, N. M., Brandshaw, J. F., Kennedy D. and Correia, J. A. 1990. The principal axes Transformation - A method for Image Registration. The Journal of Nuclear Medicine 31 (10): 1717-1722.

[2]   Althof, R. J., Wind M. G. J. and Dobbins, J. T. III. 1997. A Rapid and Automatic Image Registration Algorithm with Subpixel Accuracy. IEEE Transactions on Medical Imaging, Vol. 16. No. 3.

[3]   Atkinson, D., Hill, D. L. G., Stoyle, P. N. R., Summers, P. E. and Keevil, S. F. 1997. Automatic Correction of Motion Artifacts in Magnetic Resonance Images Using and Entropy Focus Criterion. IEEE Transactions on Medical Imaging, Vol. 16, No. 6.

[4]   Arendsen R. and Bentum M. 1991. Design and realization of computer system for high speed single exposure dual-energy image processing. Master Thesis, University of Twente, Netherlands.

[5]   Bellers, E. B. and De Bruijn F. J. 1993. On the automation of single exposure dual-energy computed-radiography. Master Thesis. University of Twente, Netherlands.

[6]   Besl, P. J. and McKay, N. D. 1992. A Method for Registration of 3-D Shapes. IEEE Transactions on Pattern Analysis and Machine Intelligence, Vol. 14, No.2.

[7]   Biswal, B. B. and Hyde, J. S. 1997. Contour-Based Registration Technique to Differentiate Between Task-Activated and Head Motion-Induced Signal Variations in fMRI. MRM 38: 470-476.

[8]   Chiang, J. Y. and Sullivan, B. J. 1993. Coincident Bit Counting – A New Criterion for Image Registration. IEEE Transactions on Medical Imaging, Vol. 12, No. 1.

[9]   Cideciyan, A. V., Jacobson, S. G., Kemp, C. M., Knighton, R. W. and Nagel J. H. 1992. Registration of high resolution images of the retina. SPIE Vol. 1652 Medical ImagingVI: Image Processing.

[10]   Carlo Ciulla, Tsunehiro Takeda and Hiroshi Endo. 1999. MEG characterization of spontaneous Alpha Rhythm in the Human Brain. Brain Topography, 11 (3): 211-222.

[11]   Ciulla, C., Takeda, T., Morabito, M., Endo, H., Kumagai, T. and Xiao R. 1996. MEG measurements of 40Hz auditory evoked response in human brain. Visualization of Information Processing in the Human Brain: Recent advances in MEG and Functional MRI. EEG Suppl. 47.

[12]   Cox, R. W. 1996. AFNI: Software for analysis and Visualization of Functional Magnetic Resonance Neuroimages. Computer and Biomedical Research, 29: 162-173.

[13]   De Castro, E. and Morandi, C. 1987. Registration of Translated and Rotated Images Using Finite Fourier Transforms. IEEE Transactions on Pattern Analysis and Machine Intelligence. Vol. PAMI-9. No. 5.

[14] Eddy, W. E., Fitzgerald, M. and Noll, D. C. 1996. Improved Image Registration by Using Fourier Interpolation. MRM 36: 923-931.

[15] Demmel, J. W. 1997. Applied Numerical Linear Algebra. SIAM, Society for Industrial and Applied Mathematics, 195-264.

[16] Dobbins, J. T. III, Rice J. J. Goodman, P. C., Patz, E. F. Jr., and Ravin, C. E. 1993. Variable Compensation chest radiography performed with a computed radiography system: Design, considerations and initial clinical experience. Radiol., Vol. 187, pp 55-63.

[17] Friston, K. J., Williams, S., Howard, R., Frackowiak, R. S. J. and Turner R 1996. Movement-Related Effects in fMRI Time Series. Magnetic Resonance in Medicine 35: 346-355.

[18] Lee, C. C., Jack, C. R. Jr., Grimm, R. C., Rossman, P. J., Felmlee, J. P., Ehman, R. L. and Riederer, S. J. 1996. Real-Time Adaptive Motion Correction in Functional MRI. MRM 36: 436-444.

[19] Lee, C. C., Grimm, R. C., Manduca, A., Felmlee, J. P., Ehman, R. L., Riederer, S. J. and Jack, C. R. Jr. 1998. A Prospective Approach to Correct for Inter-Image Head Rotation in FMRI. MRM 39: 234-243.

[20] Maas, L. C., Frederick, Blaise deB., and Renshaw, P. F. 1997. Decoupled Automated Rotational and Translational Registration for Functional MRI Time Series Data: The DART Registration Algorithm. MRM 37: 131-139.

[21] Pellizzari, C. A., Chen, G. T. Y., Spelbring, D. R., Weichselbaum R. R. and Chin-Tu C. 1989. Accurate Three-Dimensional Registration of CT, PET, and/or MR Images of the Brain. Journal of Computer Assisted Tomography

13 (1): 20-26.

[22]   Powell, M. J. D. 1964. An efficient method for finding the minimum of a function of several variables without calculating derivatives. Comput. J. 7: 155-63.

[23]   Pratt, W. K. 1974. Correlation Techniques of Image Registration. IEEE Transactions on Aerospace and Electronic Systems. AES-10 (3): 353-358.

[24]   Woods, R. P., Mazziotta, J. C. and Cherry, S. R. 1993. MRI - PET Registration with Automated Algorithm. Journal of Computer Assisted Tomography. 17 (4): 536-546.

[25]   Woods, R. P., Cherry, S. R. and Mazziotta, J. C. 1992. Rapid Automated Algorithm for Aligning and Reslicing PET Images. Journal of Computer Assisted Tomography. 16 (4): 620-633.